POLITECNICO DI TORINO
Repository ISTITUZIONALE

# A Review on Different Techniques of Mutual Coupling Reduction Between Elements of Any MIMO Antenna. Part 1: DGSs and Parasitic Structures

*Original*
A Review on Different Techniques of Mutual Coupling Reduction Between Elements of Any MIMO Antenna. Part 1: DGSs and Parasitic Structures / Kumar, A., Ansari, A.Q., Kanaujia, B.K., Kishor, J., Matekovits, L.. - In: RADIO SCIENCE. - ISSN 0048-6604. - ELETTRONICO. - 56:3(2021). [10.1029/2020RS007122]

*Availability:*
This version is available at: 11583/2877543 since: 2021-03-27T17:56:39Z

*Publisher:*
American Geophysical Union

*Published*
DOI:10.1029/2020RS007122

*Terms of use:*

This article is made available under terms and conditions as specified in the corresponding bibliographic description in the repository

*Publisher copyright*

(Article begins on next page)

16 October 2026

Check for updates

Radio Science

REVIEW ARTICLE
10.1029/2020RS007122

**Key Points:**

- Multiple-Input-Multiple-Output (MIMO) patch antenna is required for high data rate transmission without additional bandwidth requirement
- Mutual coupling reduction among antenna elements is a significant challenge while designing a compact antenna array system
- Defected Ground Structures and Parasitics elements/structures for mutual coupling reduction have been discussed thoroughly in this article

**Correspondence to:**
L. Matekovits,
ladislau.matekovits@polito.it

**Citation:**
Kumar, A., Ansari, A. Q., Kanaujia, B. K., Kishor, J., & Matekovits, L. (2021). A review on different techniques of mutual coupling reduction between elements of any MIMO antenna. Part 1: DGSs and parasitic structures. *Radio Science*, *56*, e2020RS007122. https://doi.org/10.1029/2020RS007122

Received 30 APR 2020
Accepted 2 DEC 2020

© 2021. American Geophysical Union. All Rights Reserved.

# A Review on Different Techniques of Mutual Coupling Reduction Between Elements of Any MIMO Antenna. Part 1: DGSs and Parasitic Structures

**Amit Kumar[1], Abdul Quaiyum Ansari[2], Binod Kumar Kanaujia[3], Jugul Kishor[4], and Ladislau Matekovits[5,6,7]**

[1]Department of Electrical and Electronics Engineering, Darbhanga College of Engineering, Darbhanga Bihar, India, [2]Department of Electrical Engineering, FET, Jamia Millia Islamia, New Delhi, India, [3]School of Computational and Integrative Sciences, Jawaharlal Nehru University, New Delhi, India, [4]Department of Electronics and Communication Engineering, JIMS Engineering Management Technical Campus, Greater Noida, India, [5]Dipartimento di Elettronica e Telecomunicazioni, Politecnico di Torino, Torino, Italy, [6]Faculty of Electronics and Telecommunications, Politehnica University Timisoara, Timisoara, Romania, [7]Istituto di Elettronica e di Ingegneria dell'Informazione e delle Telecomunicazioni, National Research Council, Turin, Italy

**Abstract** This two-part article presents a review of different techniques of mutual coupling (MC) reduction. MC is a major issue when an array of antennas is densely packed. When the separation between the antennas is $<\lambda_0/2$, i.e., half of the free-space wavelength, the antenna parameters suffer from the surface wave, and the space wave coupling effect between the antenna elements. To reduce the MC influence, several techniques have been discussed in the scientific literature. This part of the review paper will discuss strategies: antenna placement and orientation approach, Defected Ground Structures (DGSs), slots/slits-etching approach, protruding ground stub structures, and parasitic elements/structures. This article concludes with feasibility, applications, and comparison of the techniques mentioned above. Simultaneously, the applications and possibilities of the remaining methods are discussed in part two of the article.

**Plain Language Summary** A comprehensive two-part review article with more than 330 references is proposed.

## 1. Introduction

With the advancement in the high data rates wireless transmission, the demand for high channel capacity planar antennas, especially for handheld devices, has shown a significant market. Multiple-Input-Multiple-Output (MIMO) antennas can fulfill the top requirement. MIMO antenna helps in increasing data throughput and link coverage without sacrificing additional bandwidth or increased transmit power (Kumar et al., 2018a, 2018b). The MIMO antenna's other advantages are: high data throughput and link range without additional spectrum requirement, increased transmit power, spatial diversity and pattern diversity, and less signal dropout (Kumar et al., 2019a). In MIMO, multiple antennas radiate simultaneously and act as a transmitter or receiver depending upon its purpose. Multiple antennas placed on a single substrate sharing at least one standard radiating frequency will be considered an MIMO antenna. The MIMO antenna should have a common ground, easing the integration with monolithic integrated circuits (ICs) (Kumar et al., 2020a). However, sometimes the MIMO antenna does not have a common ground plane, but such cases should be avoided for better integration purposes and standard voltage levels.

MIMO antenna should be more compact to have a reduced form factor. The MIMO antenna's compactness is another primary concern when multiple antennas are placed on a single substrate. If the antenna element spacing is less than the $\lambda_0/2$, i.e., half of the free-space wavelength, then the antenna suffers from the surface wave and the space wave coupling effect between the antenna elements (Dama et al., 2011). For that reason, as the compactness increases, the chances of MC effect increase, resulting in degradation in the MIMO antenna performance due to power losses in a rich scattering environment. Therefore, an effective isolation technique is a must in the design of a compact MIMO antenna. Besides this, pattern and spatial diversity

need to be taken care of while introducing any isolation techniques: it should not disturb the antenna far-field radiation pattern and the impedance matching at large.

This two-part article deals with a thorough description of the existing isolation techniques for minimizing the MC between patch antennas present until the to date literature. It clearly states the MC reduction techniques' purpose and significance between the patch antennas in an array configuration. Several methods have been introduced and published in the literature. Still, each one has its kind of resemblance and advantage depending upon the antenna's design and working under consideration and the given application. Some more specific parameters, especially of the MIMO antenna, have been thoroughly discussed (Chen, 2015; Nadeem & Choi, 2019; Paulraj et al., 2004; Stjernman, 2005; Thuwaini, 2018; Vaughan & Andersen, 1987). Many review papers (Chouhan et al., 2018; Irene & Rajesh, 2018a, 2018b; Malviya et al., 2017; Nadeem & Choi, 2019) have already been published, citing various techniques of MC reduction. However, the main objective is to have closely spaced MIMO antenna elements with high isolation between them. The techniques we will discuss in part one of the two-part articles are tabulated in Table 1.

**Table 1**
*Mutual Coupling Reduction Techniques With references*

| Techniques | References |
|---|---|
| Antenna placement and orientation approach | Aminu-Baba et al. (2019), Chu et al. (2018), Chung and Kharkovsky (2013), Huang et al. (2015a, 2015b), Karimian et al. (2012), Khan et al. (2020), Liao et al. (2015) Luo et al. (2013), Mathur and Dwari (2018a), Nirdosh et al. (2018), Ojaroudi et al. (2014), Rekha et al. (2020), Sarkar and Srivastava (2017), Srivastava et al. (2019), and Tao and Feng (2016) |
| Defected Ground Structures (DGSs) | Abbosh (2007), Abdalla and Ibrahim (2013), Abid et al. (2018), Acharjee et al. (2018), Anitha et al. (2014), Asghar et al. (2018), Breed (2008), Chen and Chang (2016), Deng et al. (2017), Dhar and Sharawi (2014), Elsheakh et al. (2010), Gao et al. (2020), Gautam et al. (2019), Ghouz (2015), Habashi et al. (2011), Hussain et al. (2018), Irene and Rajesh (2018a, 2018b), Jamal et al. (2020), Khandelwal et al. (2017), Kim et al. (2008), Kumar et al. (2020b), Li et al. (2018, 2019), Lu et al. (2018), Malviya et al. (2016b), MoradiKordalivand et al. (2014), Numan et al. (2013), Ramachandran et al. (2016), Singh et al. (2015), Wang et al. (2015), Wang et al. (2014), Webster et al. (2014), Wei et al. (2016a, 2016b, 2017), Weng et al. (2008), Wu et al. (2019), Y et al. (2020), Yang et al. (2014), Yang et al. (2020), Zhang et al. (2020) and Zhu et al. (2016) |
| Slots/slits-etching approach | Addaci et al. (2014), Ayatollahi et al. (2012), Bhanumathi and Sivaranjani (2019), Biswal and Das (2018b), Chiu et al. (2007), Fritz-Andrade et al. (2020), Gangwar et al. (2020), Huang et al. (2015a), Hussain et al. (2019), Ikram et al. (2018), Jaglan et al. (2018, 2017), Jetti and Nandanavanam (2018), Kang et al. (2016), Khan et al. (2017b), Li et al. (2009), Liu et al. (2015), Lu et al. (2011), Marzudi et al. (2015), Nandi and Mohan (2017), Nirmal et al. (2019), Ouyang et al. (2011), Park et al. (2012), Ren et al. (2014), Sharawi et al. (2012), Sonkki and Salonen (2010), Srivastava et al. (2016), Srivastava and Mohan (2015), Ul Haq and Koziel (2018), Wang et al. (2020), Wu and Chu (2014), Zhou et al. (2012), Yang et al. (2016), Yang et al. (2018), Zhai et al. (2013), Zhang et al. (2015), Zhang et al. (2012), and Zuo et al. (2010) |
| Protruding ground stub structures | Ban et al. (2014), Bhattacharya et al. (2019), Biswal and Das (2018a, 2019), Chacko et al. (2013), Chandel and Gautam (2016), Chandel et al. (2018), Dong et al. (2020), Gao et al. (2014), Gautam et al. (2018), Govindarajulu et al. (2020), Hong et al. (2008), Huang et al. (2015a), Huang and Xiao (2015), Iqbal et al. (2017), Khan et al. (2015), Khan et al. (2017a), Krishna and Kumar (2016), Kumar et al. (2019b, 2020a, 2020c, 2020d), Kumar et al. (2018c), Li et al. (2013a, 2013b), Liu et al. (2013), Malviya et al. (2016a), Mao and Chu (2014), Mathur and Dwari (2018b, 2019a, 2019b), Mchbal et al. (2018), Saxena et al. (2017), Sharawi et al. (2011), Shoaib et al. (2015, 2014), Silveira et al. (2009), Singh and Tripathi (2019), Singh et al. (2013), Srivastava and Kanuijia (2015), Toktas (2017), Wani and Vishwakarma (2016), Wu et al. (2018), Wu, Lyu, & Yu (2019); Wu, Lyu, Yu, & Xu (2019), Yadav et al. (2018), Yang et al. (2012, 2016), Yoon et al. (2011), Zeng et al. (2012), Zhang et al. (2009), Zhao et al. (2019), and Zhu et al. (2016a, 2016b) |
| Parasitic elements/structures | Addaci et al. (2012), Alsultan and Ögücü Yetkin (2018), Arun et al. (2014), Azarm et al. (2019), Caizzone (2017), Chouhan et al. (2019), Debnath et al. (2018), Faraz et al. (2019), Ghimire et al. (2019), Ghosh (2016), Ghosh and Parui (2014), Alsath et al. (2013), Hatami et al. (2019), Hwang et al. (2010), Isaac et al. (2018), Kang et al. (2015), Kang and Wong (2010), Kumar et al. (2018b, 2019a), Lee et al. (2009), Lee et al. (2012), Li et al. (2012, 2016), Mak et al. (2008), Min et al. (2005), Minz and Garg (2010), Nie et al. (2019), Park et al. (2019), Payandehjoo and Abhari (2014), Roshna et al. (2015), Sharawi et al. (2017), Sharawi (2013), Singhal (2019), Thummaluru et al. (2019), Vasu Babu and Anuradha (2020), Wang et al. (2019), Wang et al. (2016), Wen and Xin-Liang (2018), Wu et al. (2017), Liu et al. (2018), Yu et al. (2020), and Zhu et al. (2016) |

Before going into the details of different isolation techniques' performance, we should know some basic diversity performance parameter check discussed in the next section.

## 2. Mutual Coupling and Diversity Performances

### 2.1. Mutual Coupling

Mutual coupling (MC) is a physically complex phenomenon that refers to the electromagnetic interaction or the reaction between different antenna elements in a proximity configuration, as happens, e.g., in an array system. Even if all antennas are transmitting, they will simultaneously receive part of each other's transmitted energy.

A schematic diagram has been shown in Figures 1a–1c to explain the different paths through which the waves travel from one antenna to the other radiators. Figure 1a shows the various pathways through which the energy interchanges indirectly via scattering (transmission coefficients like $S_{ji}$ where $i$th is the transmitting and $j$th is the receiving antenna) between four antenna elements placed in closed proximity, resulting in MC's manifestation. Similarly, in Figure 1b, Antenna $m$ is radiating as it is connected to an active source, but the Antenna $n$ is terminated (passive) with a characteristic impedance of 50 Ω. Antenna $m$ can produce electromagnetic waves and radiate in free-space denoted by 2 in Figure 1b. Some portion of the radiated energy is received by the passive Antenna $n$ characterized by 3. Some energy is reflected back to the port represented by 1. In contrast, some part of the rescatter energy is again received by the Antenna $m$ as depicted by 4, thus expressing that the total energy is not coming from the exciting Antenna $m$ only but also from the passive Antenna $n$. Therefore, MC needs to be checked to increase the performance and save the rescattering of energy. The unwanted incident radiation induces a current in the passive antenna elements due to coupling and will disturb its radiation characteristics. According to the reciprocity theorem, the same holds in the opposite direction (inverting the transmitter and receiver antennas) since MC is a symmetric phenomenon. The energy will also be wasted if some part of the radiating patch antenna gets transferred or induced to the nearby elements. Figure 1c shows the traveling of surface wave currents through the metallic patch placed on the top. It will radiate only when there is some discontinuity, curve, or truncation in the path. There will be some decay constants based on the permittivity of the substrate's dielectric constant, which decides the direction of the surface wave currents along the substrate and will radiate along the edges, as shown in Figure 1c. This impact will be severe in an antenna array, and so the surface current distribution needs to be checked and should be prevented from reaching the nearby antenna elements. So, proper isolation of the radiating antenna elements on the same substrate should be guaranteed to improve the radiation efficiency and preserves the spatial and pattern diversity of the individual antenna elements in an antenna array system.

The MC problem frequently arises in patch antennas when >1 antenna element is placed closer than $\lambda_0/2$ on a single substrate. Usually, these antenna elements are located in an array configuration, i.e., the dif-

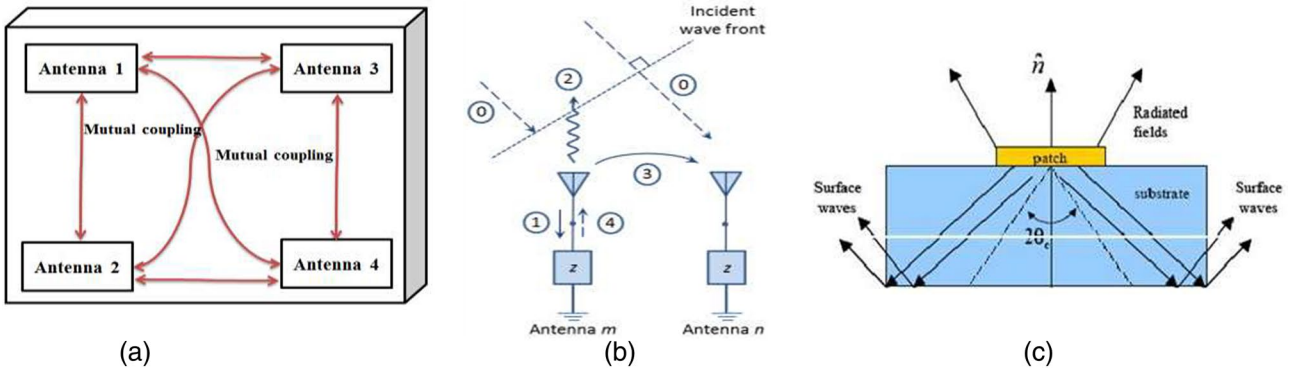


**Figure 1.** A schematic diagram illustrating the MC phenomena between compact antenna elements of any MIMO antenna (Thuwaini, 2018). MC, mutual coupling; MIMO, Multiple-Input-Multiple-Output.

ferent radiators have the same effective height. Antenna array plays a vital role in MIMO Systems (Smart Antenna Technology).

Strong MC causes:

- poor port isolation
- degradation of the spatial and pattern diversity
- reduction of antenna efficiency
- reduction of the antenna gain
- high correlation among radiators

So, we have some diversity performance check mentioned below to ensure the MIMO antenna systems' better performance.

### 2.1.1. Diversity Performances

To justify MIMO antennas performance, some of the diversity parameters, such as ECC (envelope correlation coefficient) (Chen, 2015; Kumar et al., 2018a, 2019a), DG (diversity gain) (Kumar et al., 2020a), MEG (mean effective) (Kumar et al., 2018a, 2019a), TARC (total active reflection coefficient) (Kumar et al., 2018a) and CCL (channel capacity loss) (Kumar et al., 2018a), have to be calculated and verified.

#### *2.1.1.1. ECC and DG*

The ECC describes how one antenna is correlated with other antennas present in their region of interference. Part of interference is considered an area that is coming under $\lambda_0/2$ distance from the concerned antenna resulting in MC among the antennas, and hence, it degrades the antenna performance (Dama et al., 2011). If the gap between the adjacent antennas is more than $\lambda_0/2$, it will not affect the nearby antennas; however, to achieve compactness; generally, two antennas are placed tightly. A general equation to compute ECC (Kumar et al., 2018a) is given below

$$\rho e\left(i,j,N\right)=\frac{\left|\sum_{n=1}^{N}S_{i,n}^{*}S_{n,j}\right|^{2}}{\Pi_{k=(i,j)}\left[1-\sum_{n=1}^{N}S_{i,n}^{*}S_{n,k}\right]} \tag{1}$$

Here, $i$ and $j$ are antenna elements (radiators) and $N$ is the total number of antennas taken under considerations.

The approach of calculating ECC through $S$-parameters becomes more reliable by considering the antenna elements' radiation efficiencies (Nadeem & Choi, 2019), as shown in

$$\rho_{ij.\max}=\frac{-\sum_{n=1}^{N}S_{ni}^{*}S_{nj}}{\sqrt{\left(1-\sum_{n=1}^{N}|S_{ni}|^{2}\right)\left(1-\sum_{n=1}^{N}|S_{nj}|^{2}\right)\eta_{rad.i}\eta_{rad.j}}}+\sqrt{\left(\frac{1}{\eta_{rad.i}}-1\right)\left(\frac{1}{\eta_{rad.j}}-1\right)} \tag{2}$$

where $\eta_{rad.i}$ and $\eta_{rad.j}$ are the radiation efficiencies of $i$th and $j$th antenna elements of an MIMO antenna system. But for lower efficiency antenna, the above relation gives higher values. This method is also not suitable for pattern shape or a tilted beam (Nadeem & Choi, 2019). ECC should be as low as possible, with an acceptable limit of 0.05 (Kumar et al., 2018a).

ECC of the MIMO antenna has also been calculated using the equation based on the antennas' far-field radiation patterns (Kumar et al., 2019a, 2020a), as described in 3. Envelope correlation $\rho_{ij}$ compares how the radiation pattern of the $i$th antenna element of an MIMO system is correlated with the $j$th antenna element. The calculation of ECC based on correlation coefficients from $S$-parameters gives shallow values. The computation of ECC using the $S$-parameter approach will provide you with port isolation value and is acceptable for the narrowband antenna. Still, for a wideband antenna, this approach is not so accurate. So,

in general, it is better to compute ECC from far-field radiation patterns parameters (Kumar et al., 2019a) as given in 3. The lower will be the value; the better will be the radiation pattern diversity.

In the computational approach of ECC based on far-field radiation pattern mentioned in Equation 3, XPR is the measure of the cross-polarization rate of the incident field, which is defined as $P_V/P_H$, where $P_V$ and $P_H$ are the average power along the vertical and horizontal axis of the antenna, respectively, i.e., along with the spherical coordinates $\theta$ and $\Phi$ respectively. $E_{\theta i}$ and $E_{\Phi i}$ are the complex envelopes of $\theta$ and $\Phi$ components of the radiated far-field, respectively, when only the $i$th port is excited, and other ports are terminated with 50 Ω loads. $P_\theta$ and $P_\Phi$ are the probability of distributions of the incident power on the antenna in $\theta$ and $\Phi$ directions, respectively. The solid angle $\Omega$ is the two-dimensional angle in the three-dimensional radiation pattern defined by $\theta$ in elevation and $\Phi$ in azimuth. We will consider the reference of an isotropic environment where the $P_V$ and $P_H$ are almost equal, so $XPR = 1$ and $P_\theta = P_\Phi = 1/4\pi$. While calculating ECC from far-field, value <0.5 is widely accepted, unlike 0.05, in the case of $S$-parameters

$$\rho_{ij} = \frac{\left|\int\Omega\left[XPR \cdot E_{\theta i}E^*_{\theta j}P_\theta + E_{\phi i}E^*_{\phi j}P_\phi\right]d\Omega\right|^2}{\int\Omega\left\{XPR \cdot E_{\theta i}E^*_{\theta i}P_\theta + E_{\phi i}E^*_{\phi i}P_\phi\right\}d\Omega \times \int\Omega\left\{XPR \cdot E_{\theta j}E^*_{\theta j}P_\theta + E_{\phi j}E^*_{\phi j}P_\phi\right\}d\Omega} \tag{3}$$

Another method to compute ECC by utilizing far-field radiation is given in 4, where $\eta_{max}$ is the maximum efficiency. It depends on the power distribution of the radiating elements. In this method, $\eta_i\ \eta_j$ is the total efficiency of the radiation elements

$$\left|\rho_{ij}(e)\right|^2 = 1 - \frac{\eta_{\max}}{\eta_i\eta_j} \tag{4}$$

Diversity gain states the amount of improvement obtained from MIMO compared to SISO (Single Input Single Output). It can be computed using the following relation (Kumar et al., 2020a), as given in 5. The maximum diversity gain is 10 at the 1% probability level with maximum-ratio combining, and $e_p$ is the diversity gain reduction factor due to correlation between the signals on the two antennas ($\rho_e$ is the envelope correlation coefficient)

$$DG = 10 \times e_p = 10 \times \sqrt{\left(1 - \left|0.99\rho_{ij}\right|\right)^2} \tag{5}$$

#### 2.1.1.2. MEG

MEG is one of the characterization parameters of the MIMO antenna. MEG is the figure of merit of the antenna that measures the amount of power received by the antenna elements in an MIMO environment as compared to an isotropic antenna in a fading environment (Kumar et al., 2018a, 2018b, 2019a, 2020a). If we consider the statistical environment to be uniform Rayleigh with equal vertical and horizontal power densities, then MEG can be computed using the following relation 6 (Kumar et al., 2018a). Also, the difference between any two *MEGi* should be <3 dB 7 (Kumar et al., 2018a, 2018b, 2019a, 2020a)

$$MEG_i = 0.5\left[1 - \sum_{j=1}^{N}\left|S_{ij}\right|^2\right] \tag{6}$$

also

$$MEG_i - MEG_j\ | < 3\text{db} \tag{7}$$

MEG is also calculated from the far-field radiation pattern given in 8 (Kumar et al., 2019a, 2020a), which is considered more reliable than the $S$-parameters approach. In Equation 8, $G_\theta$ and $G_\Phi$ are the power gain patterns of the antenna elements when $\theta$ is varied, and $\Phi$ is constant in case of $G_\theta$ and vice versa for $G_\Phi$ (Kumar et al., 2019a, 2020a)

$$MEG = \int_0^{2\pi}\int_0^{\pi}\left[\frac{XPR}{1+XPR}G_\theta(\theta,\phi)P_\theta(\theta,\phi) + \frac{1}{1+XPR}G_\phi(\theta,\phi)P_\phi(\theta,\phi)\right]\sin\theta d\theta d\phi \quad (8)$$

In an outdoor uniform propagation environment (Kumar et al., 2019a), MEG has been calculated for $XPR = 0$. Theoretically, MEG's maximum possible value is −3 dB when antenna efficiency is 100% (Kumar et al., 2020a). The difference in MEGs in dB should be close to unity and should not exceed 3 dB, as shown in 7 for better diversity performance.

#### 2.1.1.3. TARC

TARC is an important parameter to characterize MIMO antenna frequency bandwidth and radiation performance under the diverse nature of MIMO antennas (Kumar et al., 2018a, 2018b, 2019a, 2020a). It signifies the importance of impedance bandwidth and nonvarying resonance frequency even when the input signal phase $\theta$ changes for all the input ports. A generalized equation of TARC has been defined for multiple-port MIMO antenna combining all scattering parameters when the antenna is linearly polarized after considering the TARC formulation given in 9 (Irene & Rajesh, 2018a, 2018b; Kumar et al., 2018a)

$$TARC = \frac{\sqrt{\sum_{i=1}^{N}\left|S_{i1} + \sum_{m=2}^{N} S_{im}e^{j\theta_{m-1}}\right|^2}}{\sqrt{N}} \quad (9)$$

#### 2.1.1.4. CCL

CCL is one of the vital diversity performance check-up parameters for MIMO antennas. CCL helps in signifying the maximum attainable limit of message transmission rate up to which signal can be transmitted continuously over the communication channel with a loss of fewer than 0.4 bits/s/Hz over the operating frequency range (Kumar et al., 2018a, 2018b, 2019a, 2020a). It can be computed using the following Equation 10:

$$C_{loss} = -\log_2 \det\left(\alpha^R\right) \quad (10)$$

where $\alpha^R = \begin{bmatrix} \alpha_{11} & \alpha_{12} & \alpha_{13} & \alpha_{14} \\ \alpha_{21} & \alpha_{22} & \alpha_{23} & \alpha_{24} \\ \alpha_{31} & \alpha_{32} & \alpha_{33} & \alpha_{34} \\ \alpha_{41} & \alpha_{42} & \alpha_{43} & \alpha_{44} \end{bmatrix}$

where $\alpha_{ii} = 1 - \left(\sum_{j=1}^{N}\left|S_{ij}\right|^2\right)$ and $\alpha_{ij} = -\left(S_{ii}^{*}S_{ij} + S_{ji}^{*}S_{ij}\right)$

## 3. Isolation Techniques Discussion

### 3.1. Antenna Placement and Orientation Approach

On several occasions, antenna placement and their orientation are sufficient enough to achieve the minimum required isolation of 10 dB or more. But sometimes, the only disadvantage is the wastage of the substrate area and the antenna area due to an orthogonal or diagonal arrangement of the antenna elements. Like in Huang et al. (2015b) as represented in Figure 2a, the orthogonal arrangement resulted in >20 dB similarly 15 dB isolation (Tao & Feng, 2016) over the entire ultrawideband (UWB) frequency range, without any isolation/decoupling structure. Again, in Karimian et al. (2012), orthogonally placed four antenna elements achieved polarization diversity along with minimum isolation of 16 dB with the additional help of slits etched in the ground plane. In Liao et al. (2015), the four inverted-F antenna elements are arranged in a rotational symmetry as represented in Figure 2b along the square substrate's four corners to

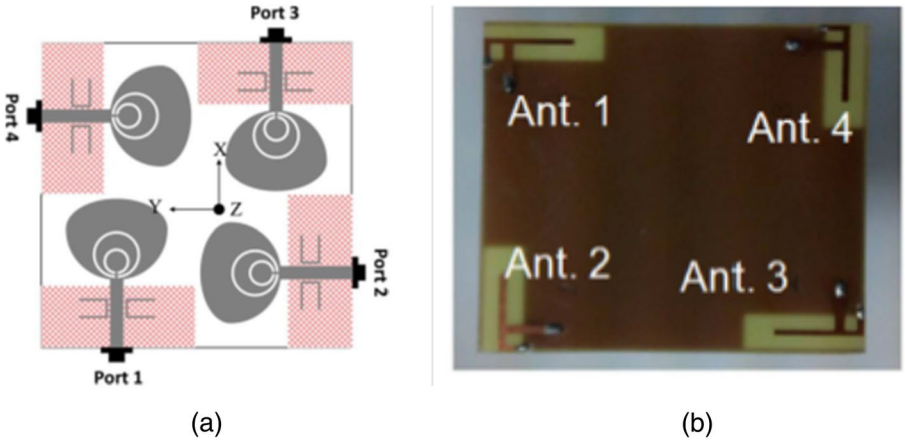


**Figure 2.** (a) Orthogonal arrangement (Huang et al., 2015b) and (b) rotational symmetry (Liao et al., 2015).

achieve decent isolation. Similar orthogonal arrangements of four elements have been shown in Chung and Kharkovsky (2013), Luo et al. (2013), Mathur and Dwari (2018a), Nirdosh et al. (2018), Sarkar and Srivastava (2017); and Srivastava et al. (2019), while in Chung and Kharkovsky (2013), there is an additional offset of 135° from the conventional sequential rotational array (SRA) for better isolation as represented in Figures 3a–3c. Some more examples of the orthogonal arrangement of two antenna elements have been shown (Aminu-Baba et al., 2019; Chu et al., 2018; Ojaroudi et al., 2014).

In Table 2, all antenna elements are orthogonally placed, minimizing the MC and attaining spatial and pattern diversity. Among all (Srivastava et al., 2019) is the most compact MIMO antenna with better isolation considering the four antenna elements.

### 3.2. Defected Ground Structures (DGSs)

Defected ground structures are the most popular technique, especially in MC reduction between wideband and ultrawideband MIMO antenna elements. Several review papers (Breed, 2008; Khandelwal et al., 2017;

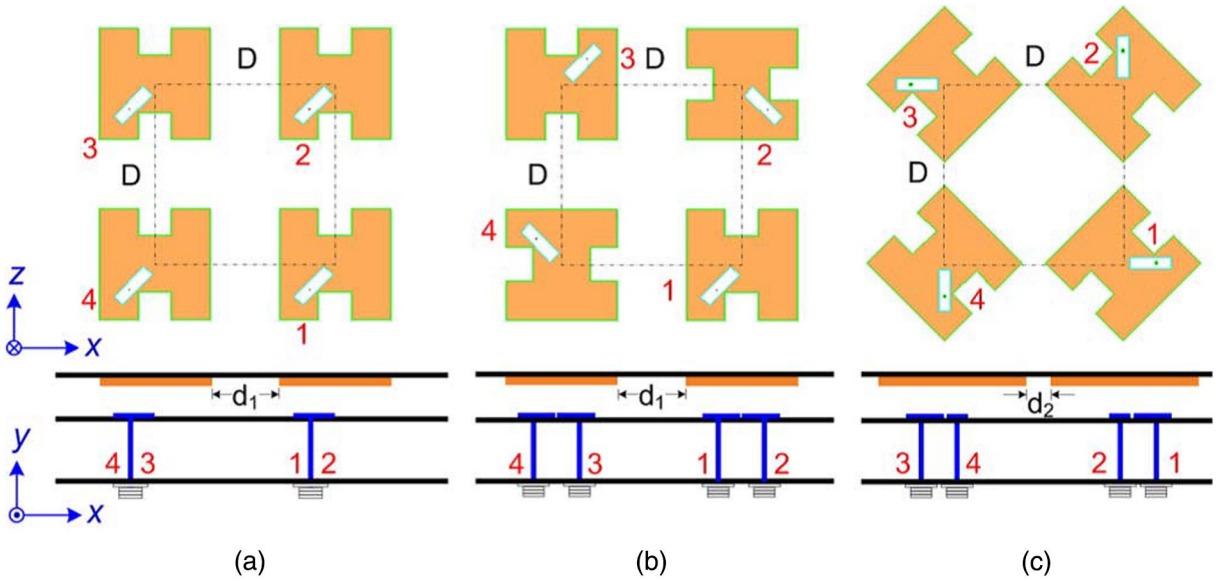


**Figure 3.** (a) Nonrotated array, (b) normal-H oriented SRA, (c) 135° angular offset. (Chung & Kharkovsky, 2013). SRA, sequential rotational array.

**Table 2**
*Comparison Between Orthogonal Antenna Elements in an MIMO Antenna Design*

| Reference | Substrate area (l × b) mm$^2$, $\lambda_0 \times \lambda_0 = \lambda_0^2$ | Min. isolation (dB) | Max. ECC value and computation approach | Antenna orientation | No. of antenna elements |
|---|---|---|---|---|---|
| Huang (2015b) | 60 × 60, 0.56 × 0.56 = 0.31 | 20 | 0.035, *S*-parameters | Orthogonal | 4 |
| Karimian et al. (2012) | 84 × 76, 0.67 × 0.61 = 0.41 | 16 | 0.05, *S*-parameters | Orthogonal | 4 |
| Liao et al. (2015) | 50 × 50, 0.41 × 0.41 = 0.17 | 16 | 0.0576, far-field | Orthogonal | 4 |
| Sarkar and Srivastava (2017) | 40 × 40, 0.32 × 0.32 = 0.10 | 14 | 0.05, — | Orthogonal | 4 |
| Luo et al. (2013) | 42 × 42, 0.71 × 0.71 = 0.50 | 17 | — | Orthogonal | 4 |
| Srivastava et al. (2019) | 87 × 81, 0.22 × 0.21 = 0.05 | 20 | 0.10, *S*-parameters | Orthogonal | 4 |
| Mathur and Dwari (2018a) | 36 × 36, 0.37 × 0.37 = 0.14 | 15 | 0.03, — | Orthogonal | 4 |
| Nirdosh et al. (2018) | 25 × 25, 0.65 × 0.65 = 0.42 | 15 | 0.14, *S*-parameters | Orthogonal | 4 |
| Chu et al. (2018) | 20 × 20, 1.87 × 1.87 = 3.50 | — | 0.0015, *S*-parameters | Orthogonal | 2 |
| Aminu-Baba et al. (2019) | 58 × 45, 0.46 × 0.36 = 0.17 | 32 | —, — | Orthogonal | 2 |

where $\lambda_0$ is the free-space wavelength at the lowest operating frequency.

Webster et al., 2014; Weng et al., 2008) are available on DGSs in the existing literature to showcase its importance during MIMO antenna designing. DGS indicates a defect in a ground plane, introduced at will, which intensely disturbs the surface current distribution on the ground plane. As a result, the impedance of the equivalent transmission line between the different antennas will change.

A rectangular ground slot has been modified in MoradiKordalivand et al. (2014) by introducing four slots, one in each corner, while a V-shaped ground branch has been introduced in (Wang et al., 2015) to decrease the spatial coupling. As represented in Figure 4a, four interdigital structures have been etched in the ground to achieve isolation of about 28 dB between the four-port MIMO antenna (Ramachandran et al., 2016). Similarly, in Deng et al. (2017), a meandering resonant branch and an inverted T-slot, as represented in Figure 4b, have been etched in the ground plane to achieve isolation in the higher and the lower bands, respectively.

A fragmented type ground plane (Wang et al., 2014) as represented in Figure 4c, a modified dumbbell-shaped DGS (Numan et al., 2013), three rectangular slots etched in the ground plane (Irene & Rajesh, 2018a, 2018b), Y-shaped DGS (Zhu et al., 2016), partially connected two rectangular slots in one case, while two crossed rectangular slots in another trial (Ghouz, 2015), modified $\pi$-shaped strip and two shorted T-shaped strips (Wu et al., 2019) as represented in Figure 5a, a funnel-shaped ground plane with an open-ended slot (Gautam et al., 2019) as depicted in Figure 5b, dumbbell-shaped modified CSSR DGS (Kumar et al., 2020b), as

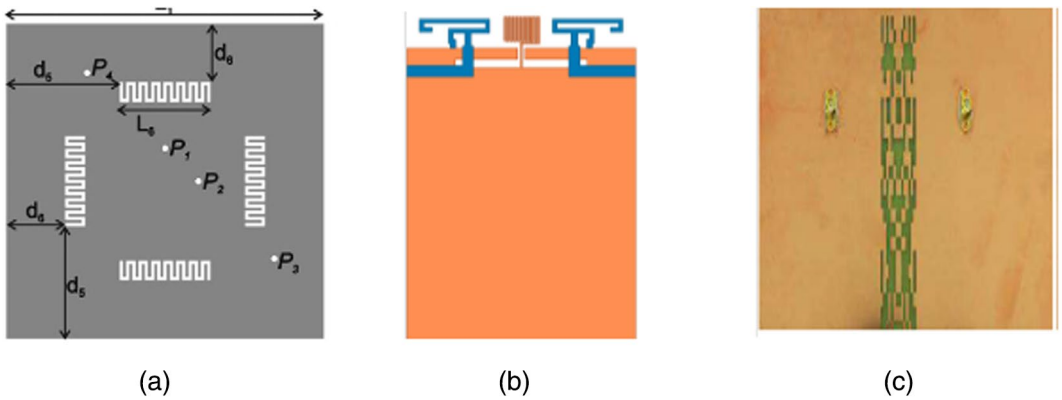


**Figure 4.** (a) Interdigital loaded ground plane (Ramachandran et al., 2016), (b) Meandering Branch and inverted T-shaped ground structure (Deng et al., 2017), and (c) fragmented type ground plane (Wang et al., 2014).

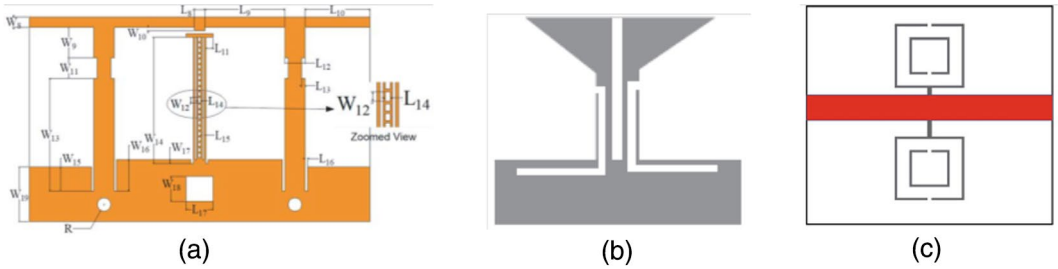


**Figure 5.** (a) Shorted T-shaped and π-shaped DGS (Wu et al., 2019), (b) funnel-shaped DGS (Gautam et al., 2019), (c) dumbbell-shaped complementary-split-ring resonator (CSRR) DGS (Kumar et al., 2020b). DGS, Defected Ground Structures.

represented in Figure 5c, T-stub loaded DGS (Y et al., 2020), U-shaped modified ground plane embedded with T-shaped slot (Li et al., 2019), a novel fractal DGS (FDGS) (Wei et al., 2016a) as represented in Figure 6a, partially stepped ground (PSG) (Malviya et al., 2016b), H-dumbbell-shaped DGS (Abbosh, 2007; Acharjee et al., 2018) shown in Figure 6b, a ladder-shaped modified ground plane (Asghar et al., 2018) shown in Figure 6c, compact DGS filtering structure (Abdalla & Ibrahim, 2013), square ring DGS (Anitha et al., 2014), meandered DGS (Chen & Chang, 2016; Dhar & Sharawi, 2014), different shapes of DGSs (Elsheakh et al., 2010) as represented in Figure 7, slotted ground plane (Abid et al., 2018), two columns of folded split-ring resonator (FSRR) etched in the ground plane Habashi et al. (2011) as represented in Figure 8a, annular slots etched DGS (Hussain et al., 2018), a $\lambda/4$ stub filter along with supplemental ground structure (Kim et al., 2008), fragmented structured DGS (Lu et al., 2018), shorted meandered line type DGS (Li et al., 2018) as represented in Figure 8b, forked shaped etched slot DGS (Singh et al., 2015), S-shaped periodic DGS (Wei et al., 2016b) as depicted in Figure 8c, another periodic spiral-shaped DGS (Wei et al., 2017)

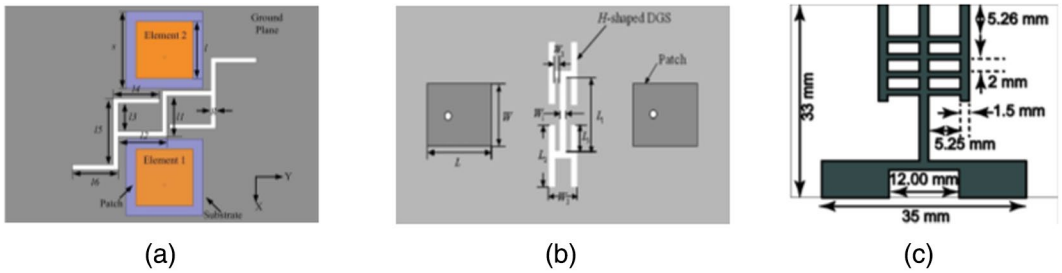


**Figure 6.** (a) FDGS (Wei et al., 2016a), (b) H-dumbbell-shaped DGS (Abbosh, 2007; Acharjee et al., 2018), and (c) ladder-shaped DGS (Asghar et al., 2018). FDGS, fractal Defected Ground Structures.

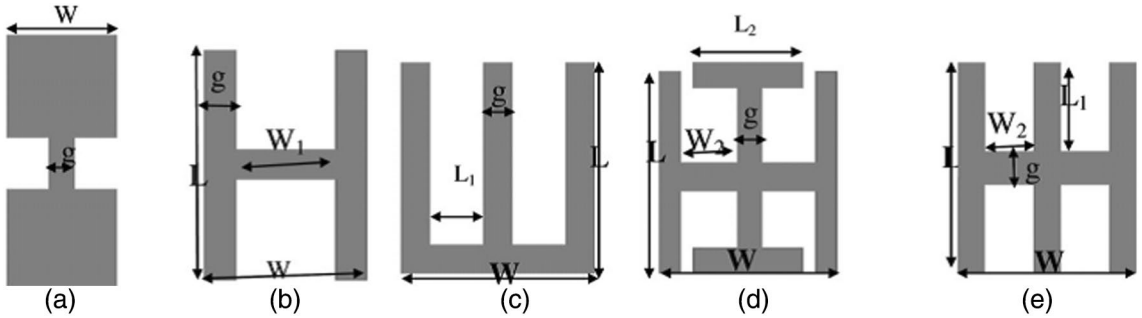


**Figure 7.** Different shapes of DGSs (Elsheakh et al., 2010). DGSs, Defected Ground Structures.

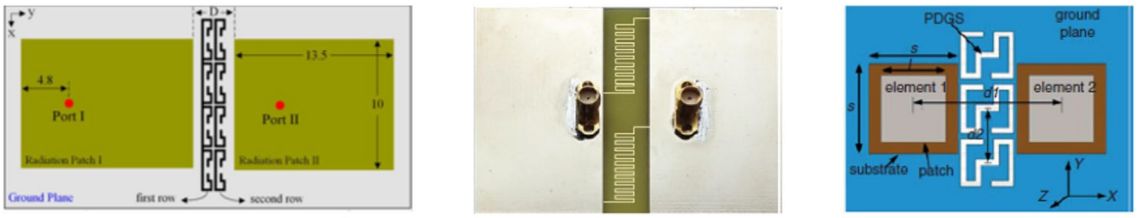


**Figure 8.** (a) Two columns of FSRRs (Habashi et al., 2011), (b) shorted meandered (Li et al., 2018), and (c) S-shaped DGS (Wei et al., 2016b). FSRRs, folded split-ring resonators.

and slotted CSRR etched DGS (Yang et al., 2014) have been used in the existing literature to isolate the elements of the tightly packed MIMO antenna.

As reported in Table 3, most wideband/UWB-MIMO antennas find difficulty in isolation than the narrowband counterpart. Among all, the MIMO antenna (Gautam et al., 2019) is the most compact one having a substrate area of 0.035 $\lambda_0^2$ only.

We can also observe that the maximum ECC value is 0.3, which is calculated from the far-field patterns irrespective of the lowest ECC value, 0.01 computed with *S*-parameters' help. The far-field computational ECC reflects pattern/spatial diversity irrespective of only port isolation when computed with *S*-parameters. So, ECC calculated from far-field is considered more accurate and reliable, especially in the wideband/UWB-MIMO antenna.

### 3.3. Slots/Slits-Etching Approach

Slots/slits-etching approach is one of the cases of DGSs. The ground has been detected by etching slots/slits in the ground plane. This approach is disturbing the flow of the surface current distributions by diverting

**Table 3**
*Comparison of MIMO Antennas Based on DGSs*

| References | Substrate area (l × b) mm$^2$, $\lambda_0 \times \lambda_0 = \lambda_0^2$ | Min. isolation (dB) | Max. ECC value and computation approach | Type of defects in the ground plane | No. of elements | Narrowband/wideband/UWB |
|---|---|---|---|---|---|---|
| Webster et al. (2014) | 40 × 40, 0.31 × 0.31 = 0.10 | 10 | 0.266, far-field | V-shaped | 4 | Wideband |
| Ramachandran et al. (2016) | 61 × 61, 0.50 × 0.50 = 0.25 | 28 | 0.300, far-field | Interdigital structure | 4 | Narrowband |
| Deng et al. (2017) | 77.5 × 52, 0.62 × 0.42 = 0.26 | 15 | 0.200, far-field | Meandering Branch and inverted T-shaped | 2 | Narrowband (dual-band) |
| Wang et al. (2014) | 120 × 197, 0.38 × 0.62 = 0.24 | 47 | ~0, *S*-parameters | Fragmented type | 2 | Narrowband |
| Wu et al. (2019) | 50 × 30, 0.39 × 0.24 = 0.09 | 24 | 0.027, *S*-parameter | $\pi$-shaped DGS | 2 | Narrowband (dual-band) |
| Gautam et al. (2019) | 15 × 26, 0.14 × 0.25 = 0.04 | 21 | 0.01, *S*-parameter | Funnel-shaped | 2 | UWB |
| Kumar et al. (2020b) | 32 × 34.25, 0.26 × 0.27 = 0.07 | 28 | Acts as band-stop filter | Dumbbell-shaped CSRR | 2 | Narrowband |
| Abbosh (2007) | 50 × 86, 0.88 × 1.52 = 1.34 | 30 | Acts as band-stop filter | H-dumbbell-shaped DGS | 2 | Narrowband |
| Asghar et al. (2018) | 33 × 45.5, 0.34 × 0.47 = 0.16 | 15 | —, — | Ladder-shaped DGS | 2 | UWB |
| Elsheakh et al. (2010) | 53 × 53, 0.84 × 0.84 = 0.71 | 20 | —, — | H-shaped DGS | 4 | Narrowband |
| Habashi et al. (2011) | 50 × 68, 0.87 × 1.18 = 1.03 | 56 | —, — | FSRRs | 2 | Narrowband |
| Li et al. (2018) | 78 × 60, 1.30 × 1.00 = 1.30 | 39 | —, — | Shorted meandered line | 2 | Narrowband |

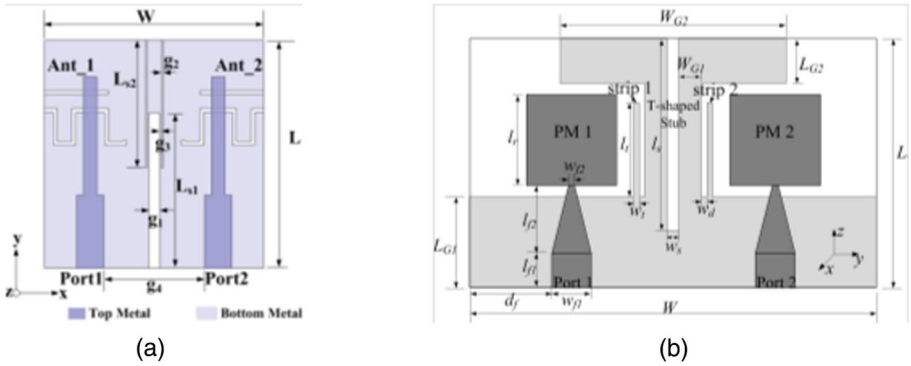


**Figure 9.** (a) One wide and two narrow slots (Nandi & Mohan, 2017) and (b) vertical slot in T-shaped stub (Liu et al., 2015).

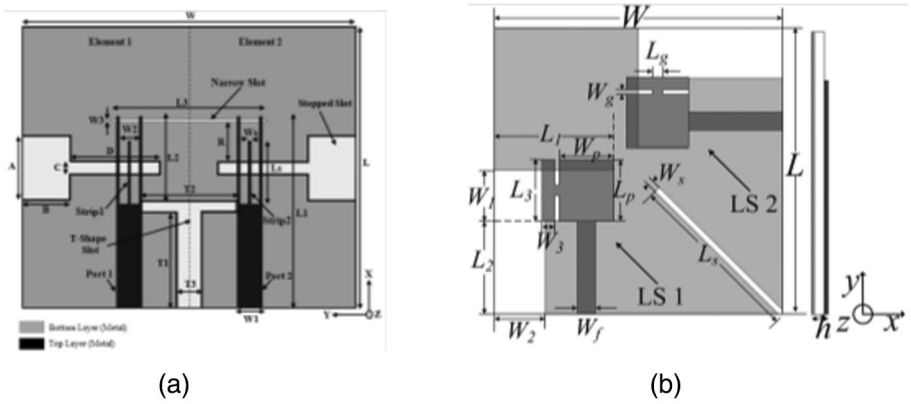


**Figure 10.** (a) One T-shaped slot and two-stepped slots (Jetti & Nandanavanam, 2018) and (b) narrow diagonal slot (Ren et al., 2014).

the conducting path. Numerous such kind of practice has been successfully reported in the existing literature. Here, some of them are going to be discussed. Even the slot etched in the common radiator helps in minimizing the MC (Khan et al., 2017b; Srivastava et al., 2016; Zhang et al., 2015). Along with the neutralization line, four slits have been etched in the ground (Yang et al., 2016) to reduce MC between the elements of the multiband MIMO antenna working for GSM, DCS, and long term evolution (LTE) indoor applications. Two slots (Addaci et al., 2014), a wide slot and a pair of narrow slots (Nandi & Mohan, 2017) as represented in Figure 9a, six slits (Jaglan et al., 2017, 2018), simple wide slot (Ouyang et al., 2011), a vertical slot along with T-shaped ground stub (Liu et al., 2015) as represented in Figure 9b, inverted T-shaped slot along with a capacitor (Park et al., 2012), one T-shaped slot and two-stepped slots (Jetti & Nandanavanam, 2018) as described in Figure 10a, a narrow slot (Ren et al., 2014) as represented in Figure 10b, slitted pattern (Chiu et al., 2007), two symmetric stepped "L"-shaped open ground slots (Biswal & Das, 2018b), T-shaped slot impedance transformer (Zhang et al., 2012), two $\lambda/4$ slots (Zuo et al., 2010), E-shaped slot on the radiator and narrow ground slot (Bhanumathi & Sivaranjani, 2019), slot line based DGS (Hussain et al., 2019), six pair of slits (Wu & Chu, 2014), n shaped slot etched below the feed-line (Ul Haq & Koziel, 2018), meandered slot (Ayatollahi et al., 2012), L-shaped slot (Huang et al., 2015a), series of slits (Li et al., 2009), four slots etched (Ikram et al., 2018), H-shaped slot (Kang et al., 2016), as represented in Figure 11a, quasi-cross-shaped slot (Lu et al., 2011), two T-slots, and a rectangular slot (Marzudi et al., 2015), as described in Figure 11b, triangular slots and meshed metal strip (Nirmal et al., 2019), again a pair of slits (Sharawi et al., 2012), two $\lambda/2$ slots (Sonkki & Salonen, 2010), cross-shaped slot and a sickle-shaped metallic strip (Srivastava & Mohan, 2015), two U-shaped slots (Zhou et al., 2012) as represented in Figure 12a, two asymmetric dumbbells

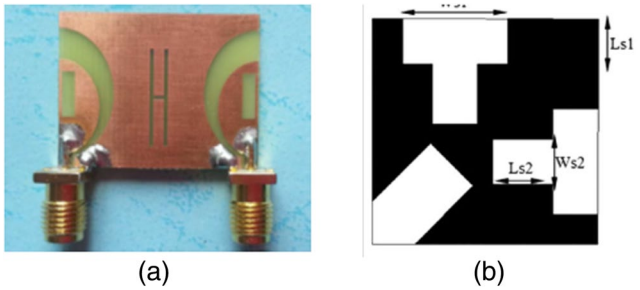


**Figure 11.** (a) H-shaped slot (Kang et al., 2016) and (b) two T-slots and one rectangular slot (Marzudi et al., 2015).

shaped slot, and one decoupling slot (Yang et al., 2018) as depicted in Figure 12b while a P-shaped slot and two F-shaped strips (Zhai et al., 2013) have been inserted in the ground plane to reduce MC.

The comparison in Table 4 shows that the slots/slits-etching process is another way of creating DGSs, which is more suitable for wideband and UWB-MIMO antenna. The maximum isolation achieved is mostly around 20 dB, unlike the cases mentioned in Table 2, where the DGSs help achieve isolation >56 dB (Habashi et al., 2011), but this holds for a narrowband MIMO antenna. Again, it has been certified that achieving better isolation in the UWB-MIMO antenna and compactness is a more significant challenge than for the narrowband MIMO antenna.

Among all, the mentioned MIMO antennas in Table 4 (Nandi & Mohan, 2017) is the most compact ($0.042\,\lambda_0^2$) UWB-MIMO antenna with 20 dB isolation.

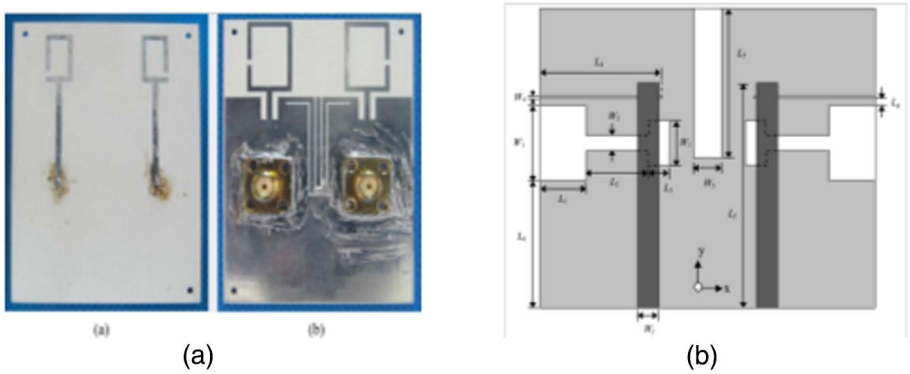


**Figure 12.** (a) U-shaped slots (Zhou et al., 2012) and (b) two dumbbells shaped and one decoupling slot (Yang et al., 2018).

**Table 4**
*Comparison of MIMO Antennas Based on Slots/Slits-Etching Approach*

| References | Substrate area (l × b) mm², $\lambda_0 \times \lambda_0 = \lambda_0^2$ | Min. isolation (dB) | Max. ECC value and computation approach | Type of slots/slits etched | No. of elements | Narrowband/ wideband/ UWB |
|---|---|---|---|---|---|---|
| Nandi and Mohan (2017) | 24 × 25, 0.20 × 0.21 = 0.04 | 20 | 0.004, *S*-parameters | One wide and two narrow slots | 2 | Narrowband (dual-band) |
| Liu et al. (2015) | 22 × 36, 0.23 × 0.37 = 0.09 | 15 | 0.1, far-field | Vertical slot in T-shaped ground stub | 2 | UWB |
| Jetti and Nandanavanam (2018) | 22 × 26, 0.23 × 0.27 = 0.06 | 20 | 0.03, *S*-parameters | One T-shaped slot and two-stepped slots | 2 | UWB |
| Ren et al. (2014) | 32 × 32, 0.33 × 0.33 = 0.11 | 15 | 0.02, *S*-parameters | Narrow diagonal slot | 2 | UWB |
| Kang et al. (2016) | 28 × 22, 0.27 × 0.21 = 0.06 | 20 | 0.03, *S*-parameters | H-shaped slot | 2 | UWB |
| Marzudi et al. (2015) | 30 × 30, 0.23 × 0.23 = 0.05 | 14 | ~0, *S*-parameters | Two T-slots and one rectangular slot | 2 | Wideband |
| Zhou et al. (2012) | 63 × 50, 0.36 × 0.28 = 0.10 | 15 | 0.01, *S*-parameters | U-shaped slots | 2 | Wideband (dual-band) |
| Yang et al. (2018) | 24 × 20, 0.25 × 0.21 = 0.05 | 18 | 0.025, *S*-parameters | Two dumbbells shaped and one decoupling slot | 2 | UWB |

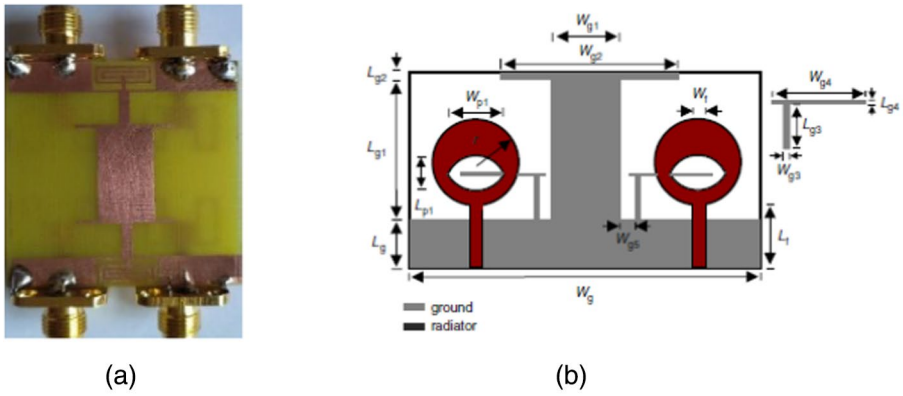


**Figure 13.** (a) Shorted T-shaped stub and CSRR (Kumar et al., 2018) and (b) T-shaped ground plane (Chandel & Gautam, 2016).

### 3.4. Protruding Ground Stub Structures

Similar to the slots/slits-etching method, protruding ground stub structures is another prevalent method of creating DGSs. It provides isolation and sometimes improves matching, and helps achieve wider impedance bandwidth (Kumar et al., 2020a). This method is prevalent in providing isolation among elements of an UWB-MIMO antenna. Some of the popular designs will be discussed here. Among all, the T-shaped ground plane structure is ubiquitous among the UWB-MIMO monopole antenna. Monopole antennas are designed with partial grounds. A T-shaped stub protruding in the middle of the MIMO antenna's ground helps to minimize the MC to a remarkable extent. Two shorted T-shaped stub and CSRR help achieve isolation of >18 dB throughout the operating frequency range, as represented in Figure 13a (Kumar et al., 2018). In Figure 13b, we can see a T-shaped ground responsible for isolation in the UWB-MIMO antenna (Chandel & Gautam, 2016). Similar to protruding almost T-shaped ground stub along with some variations like an etched slot in the T-shaped stub, stepped T-shaped stub, and more similar structures have been used in Bhattacharya et al. (2019), Huang and Xiao (2015), Kumar et al. (2020a), Li et al. (2013), Liu et al. (2013, 2015); Mathur (2019), Silveira et al. (2009), Toktas (2017), Wu et al. (2018), Wu, Lyu, & Yu (2019); Wu, Lyu, Yu, & Xu (2019); Yadav et al. (2018), Yang et al. (2012), Yang et al. (2016), and Zhao et al. (2019) for minimizing the MC among the elements of UWB-MIMO antenna. Along with a slit on the shared circular-shaped radiator, an inverted Y-shaped stub has been introduced in the ground plane at an angle of 45° (Srivastava & Kanuijia, 2015) to minimize the MC. Because of instrumental contributions of protruding ground stub structures in reducing MC particularly among wideband and UWB-MIMO antenna elements many such designs have been introduced, among those some popular designs are folded Y-shaped (Khan et al., 2015), diagonally integrated strip (Chacko et al., 2013; Gao et al., 2014), extended rectangular stub (Yoon et al., 2011), protruded I-shaped stub at an angle of 45° (Zhu et al., 2016), an inverted pair of L-shaped strips (Chandel et al., 2018; Khan et al., 2017a), an inverted L-shaped strip (Kumar et al., 2019b), tree-like stub (Zhang et al., 2009) as represented in Figure 14a, arrowhead-shaped stub at an angle of 45° (Zhu et al., 2016), an inverted L-shaped and I-shaped stub (Liu et al., 2013) as represented in Figure 14b, funnel-shaped stub (Gautam et al., 2018), circular arcs shaped stubs (Mathur & Dwari, 2018b), extended curved stub (Biswal & Das, 2019), partial ground T-shaped stub (Malviya et al., 2016a), inverted L-shaped stub integrated with T-shaped slot (Singh et al., 2013), etching T-shaped slot on the radiator and extended arrow-shaped stub (Mao & Chu, 2014), pair of extended I-shaped (Sharawi et al., 2011), a rectangular slot with one circular end embedded with two inverted-L-shaped branches (Shoaib et al., 2014), a cross-shaped stub (Singh & Tripathi, 2019), F-shaped stubs (Iqbal et al., 2017), a dual-inverted-L-shaped ground branch with a slot (Zeng et al., 2012), two protruded ground parts (Li et al., 2013), a stepped stub at an angle of 45° (Biswal & Das, 2018a), two inverted L-shaped and one I-shaped stub (Hong et al., 2008), a pair of L-stubs, spiral stubs, and L-slots (Huang et al., 2015a), narrow metallic and slot stubs (Krishna & Kumar, 2016), grounded stub along with two F-dual grounded circular ring resonator (Mathur & Dwari, 2019a) as represented in Figure 15a, two F-shaped stub and rectangular slots (Wani & Vishwakarma, 2016) as described in Figure 15b, a simple I-shaped stub (Mchbal et al., 2018), a rectangular vertical arm (Saxena et al., 2017), inverted L-shaped and slot (Shoaib et al., 2015),

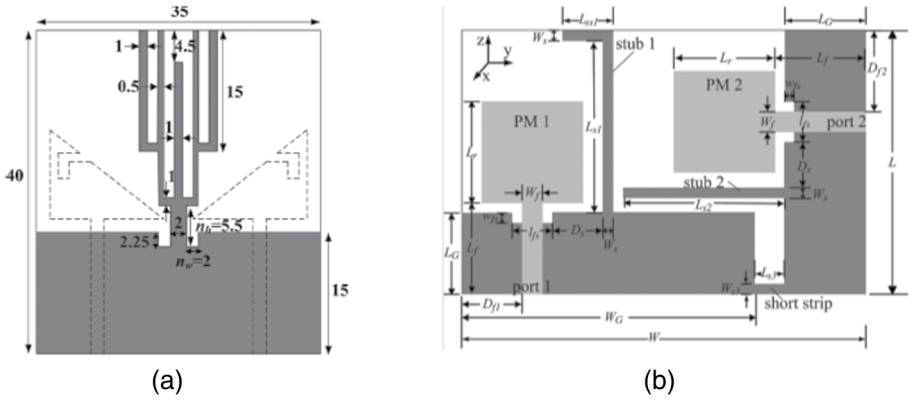


**Figure 14.** (a) Tree-like stub (Zhang et al., 2009) and (b) inverted L-shaped and I-shaped stub (Liu et al., 2013).

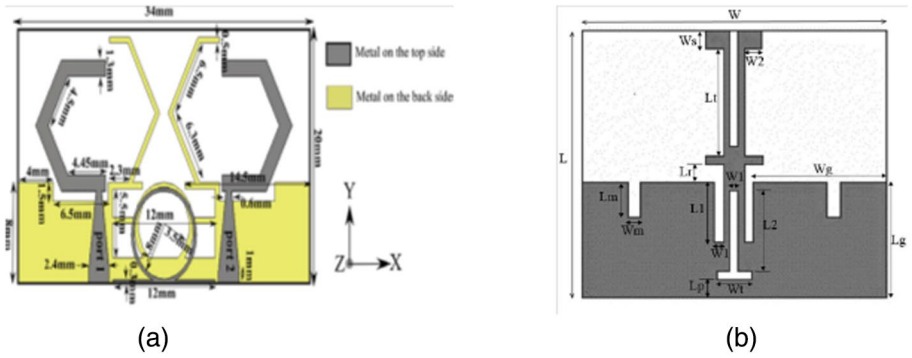


**Figure 15.** (a) Stub along with dual grounded circular ring resonator (Mathur & Dwari, 2019a) and (b) F-shaped stubs and rectangular slots (Wani & Vishwakarma, 2016).

I-shaped protruded stub (Ban et al., 2014) have been introduced in the ground plane to minimize MC and enhance the isolation among the elements of the proposed MIMO antenna.

Table 5 shows how the protruding ground stubs help in designing compact UWB-MIMO antenna having substrate area (total antenna area) almost $<0.06\,\lambda_0^2$ in most of the cases. We can also notice the lower ECC values computed by *S*-parameters than the far-field computation.

### 3.5. Parasitic Elements/Structures

In a single antenna system, the parasitic scatters are used to achieve multiresonance, which will enhance the impedance bandwidth (IBW). While in the MIMO antenna system, they are inserted between the resonating antenna as a reflector or resonator to reduce the MC between the antenna elements. Generally, parasitic elements are not connected to the ground, unlike those connected to form a sort of resonator (Sharawi, 2013). Parasitic elements will generate a coupling that will oppose the original one created by the excited antenna element. The resultant coupled field will be out of phase with the passive antenna at that moment, helping curb the effect of MC from one radiating patch to another. These elements are specifically designed to control the bandwidth of isolation and the extent of MC reduction. Many research articles have been published citing the importance of parasitic elements/structures, few we will discuss here.

A modified serpentine structure (Arun et al., 2014) occupying a width of only 3 mm, as represented in Figure 16a, has been inserted between two square patch antennas to achieve isolation as high as 34 dB at the resonating frequency of 2.45 GHz. A central metallic reflector has been placed in the center of two groups of four-elements of dielectric resonator antennas (DRAs) (Sharawi et al., 2017), as represented in

**Table 5**
*Comparison of MIMO Antenna Based on Protruding Ground Stubs*

| References | Substrate area (l × b) mm$^2$, $\lambda_0 \times \lambda_0 = \lambda_0^2$ | Min. isolation (dB) | Max. ECC value and computation approach | Type of protruding ground stub | No. of elements | Narrowband/ wideband/ UWB |
|---|---|---|---|---|---|---|
| Kumar et al. (2020a) | 19 × 30, 0.20 × 0.31 = 0.06 | 18 | 0.13, far-field | T-shaped | 2 | UWB |
| Kumar et al. (2018) | 32 × 38, 0.25 × 0.29 = 0.07 | 18 | 0.03, *S*-parameters | Shorted T-shaped stub and CSRR | 2 | UWB |
| Chandel and Gautam (2016) | 18 × 36, 0.17 × 0.35 = 0.06 | 20 | 0.012, *S*-parameters | T-shaped ground plane | 2 | UWB |
| Chandel et al. (2018) | 18 × 34, 0.18 × 0.33 = 0.06 | 22 | 0.01, *S*-parameters | Inverted L-shaped stubs | 2 | UWB |
| Khan et al. (2017a) | 23 × 29, 0.23 × 0.29 = 0.07 | 15 | 0.15, far-field | Inverted L-shaped stubs | 2 | UWB |
| Zhang et al. (2009) | 35 × 40, 0.36 × 0.41 = 0.15 | 16 | 0.01, *S*-parameters | Tree-like stub | 2 | UWB |
| Liu et al. (2013) | 26 × 40, 0.27 × 0.41 = 0.11 | 15 | 0.2, far-field | Inverted L and I-shaped Stub | 2 | UWB |
| Iqbal et al. (2017) | 50 × 30, 0.42 × 0.25 = 0.11 | 20 | 0.04, *S*-parameters | F-shaped stubs | 2 | UWB |
| Li et al. (2013) | 20 × 34, 0.20 × 0.34 = 0.07 | 20 | 0.3, far-field | Stub along with dual grounded circular ring resonator | 2 | UWB |
| Wani and Vishwakarma (2016) | 35 × 30, 0.36 × 0.31 = 0.11 | 22 | 0.005, *S*-parameters | F-shaped stubs and rectangular slots | 2 | UWB |

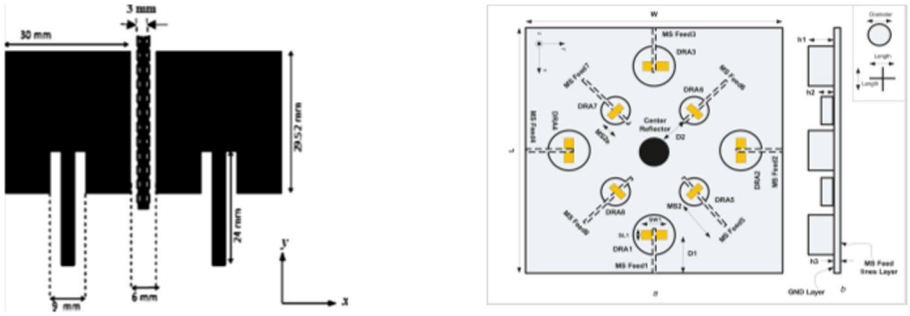


**Figure 16.** (a) Modified serpentine structure (Arun et al., 2014) and (b) center metallic reflector (Sharawi et al., 2017).

Figure 16b for isolation and tilting the radiation pattern of one group resonating at 5.8 GHz by 45° as compared to another group resonating at 2.45 GHz. Similarly, a simple metallic strip (Roshna et al., 2015), T-shaped parasitic strip (Kang et al., 2015), a modified interdigital capacitor (Kumar et al., 2018b), a novel ITI-shaped parasitic structure (Kumar et al., 2019a), parasitic inverted L-element with an open stub (Lee et al., 2012), H-shaped strip (Li et al., 2016), floating parasitic decoupling structure (Khan et al., 2014), a rotated "+" shaped rectangular strip pair (Singhal, 2019) as represented in Figure 17a, a rectangular parasitic element is embedded at the substrate backside (Hatami et al., 2019), two separate rectangular shapes and T-shaped parasitic elements (Faraz et al., 2019), as represented in Figure 17b, cross-shaped metallic fence (Caizzone, 2017), stepped cross-shaped reflector strip (Thummaluru et al., 2019), a circular parasitic element at the backside of the radiating patch (Ghimire et al., 2019), a novel reversed S-shaped walls (Wang et al., 2019), a decoupling metal strip loaded with an inductor (Nie et al., 2019), an optimized parasitic element (Addaci et al., 2012) as represented in Figure 18a, slotted meander-line resonator (SMLR) (Alsath et al., 2013) as represented in Figure 18b, a simple rectangular parasitic structure at the back (Azarm et al., 2019), diagonal parasitic strip at the back (Chouhan et al., 2019), Minkowski fractal-shaped isolators (Debnath et al., 2018) as represented in Figure 19a, a complementary pattern (CP) comprised of meandered transmission lines (Hwang et al., 2010), a group of six parasitic elements (Min et al., 2005), as represented in Figure 19b, two parallel strips, or a single strip embedded with patterned meander-shaped slot (Isaac et al., 2018) as represented in Figures 20a and 20b, two parasitic monopole providing a decoupling path

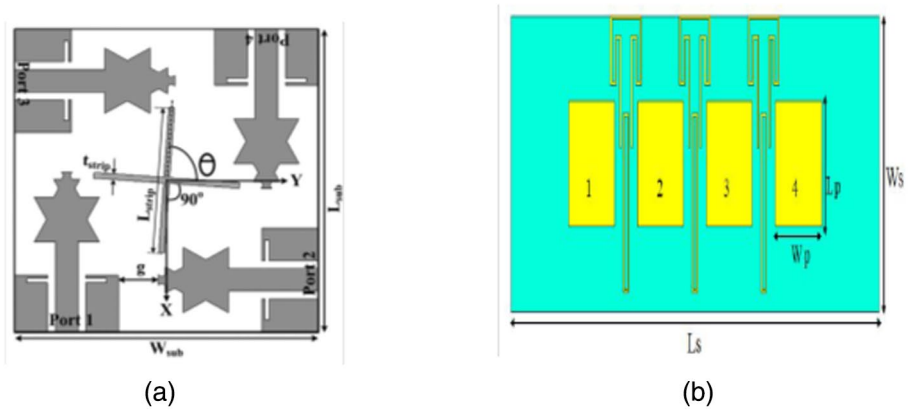


**Figure 17.** (a) Rotated "+" shaped rectangular strip pair (Singhal, 2019) and (b) two separate rectangular shape and T-shaped parasitic elements (Faraz et al., 2019).

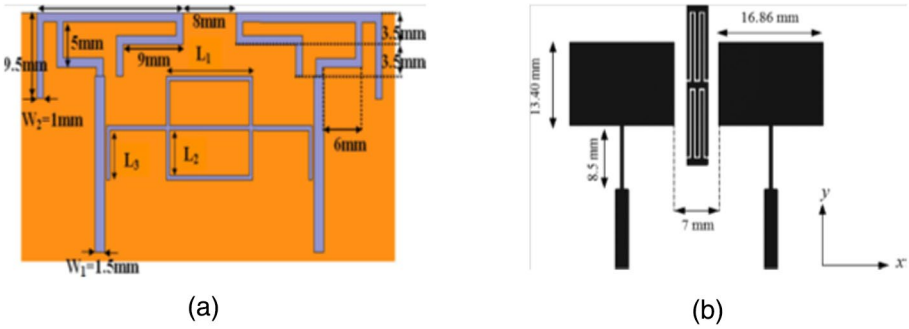


**Figure 18.** (a) Optimized parasitic element (Addaci et al., 2012) and (b) slotted meander-line resonator (SMLR) (Alsath et al., 2013).

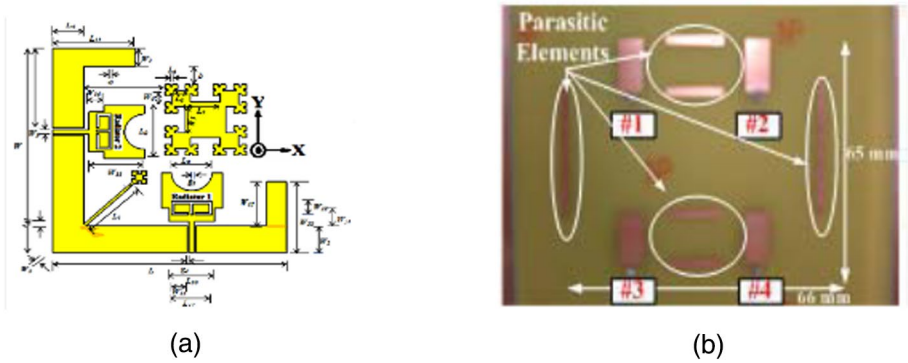


**Figure 19.** (a) Minkowski fractal-shaped isolators (Debnath et al., 2018) and (b) a group of six parasitic elements (Min et al., 2005).

(Li et al., 2012) as represented in Figure 21a, a novel H-shape parasitic element embedded in the ground plane (Liu et al., 2018) as represented in Figure 21b, a T-shaped coupling element providing an additional decoupling path (Mak et al., 2008) as represented in Figure 22a, 2 × 3 matrices of the C-shaped resonator is proposed (Alsultan & Ögücü Yetkin, 2018) as represented in Figure 22b, parasitic fragment-type isolation element (Wang et al., 2016) as represented in Figure 23a and a periodic paperclip-shaped structure (Wen & Xin-Liang, 2018) as represented in Figure 23b have been employed among patch antennas to minimize the MC between them. Further, Payandehjoo and Abhari have presented a comprehensive investigation

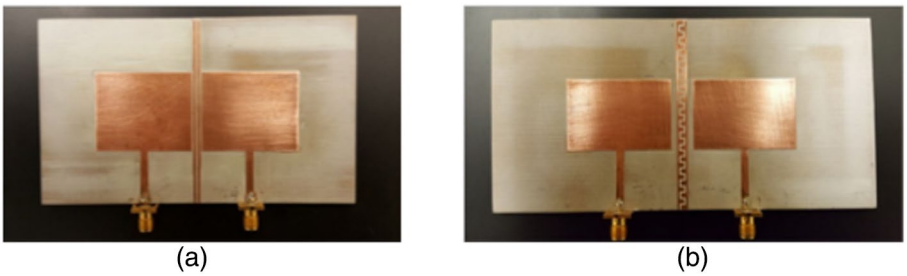

**Figure 20.** (a) Two parallel metallic strip and (b) single strip embedded with a meander-shaped slot pattern (Isaac et al., 2018).

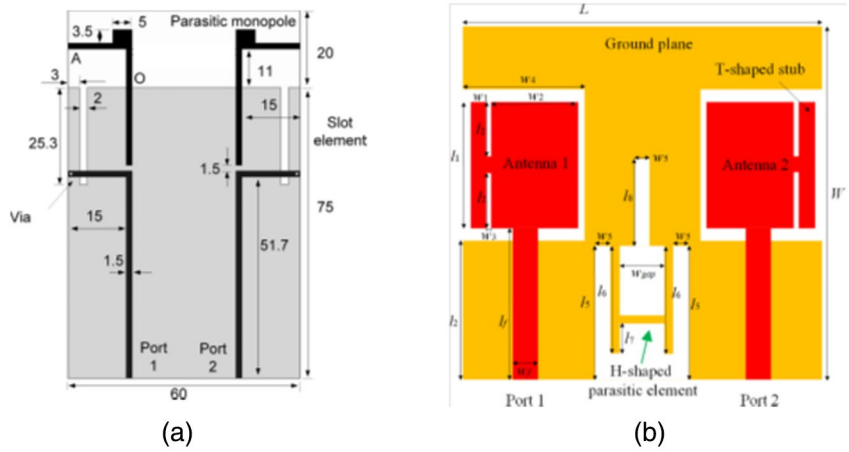


**Figure 21.** (a) Two parasitic monopole (Li et al., 2012) and (b) novel H-shaped parasitic element embedded in the ground plane (Liu et al., 2018).

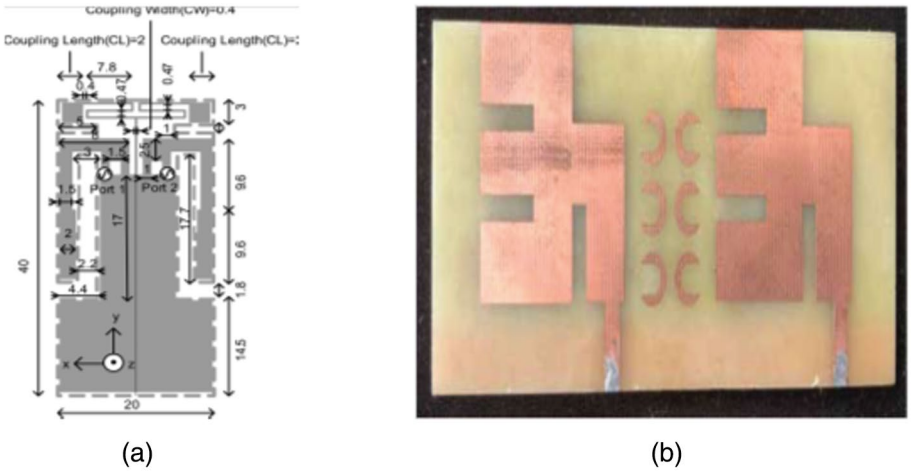


**Figure 22.** (a) A T-shaped coupling element (Mak et al., 2008) and (b) 2 × 3 matrix of C-shaped resonator (Alsultan & Ögücü Yetkin, 2018).

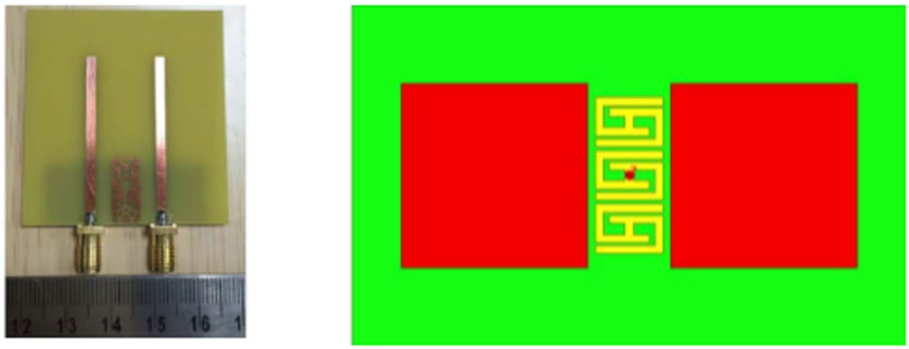

(a) (b)

**Figure 23.** (a) Parasitic fragment-type isolation element (Wang et al., 2016) and (b) periodic paperclip-shaped structure (Wen & Xin-Liang, 2018).

of parasitic elements for coupling reduction in multiband antenna for handheld devices (Payandehjoo & Abhari, 2014).

In many cases, the parasitic elements/structures will act as a resonator, which will scatter the signal coming from one antenna and thus reduces MC like two resonators have been placed between the two planar inverted-F antenna (PIFA) (Minz & Garg, 2010), a diamond-shaped patterned ground resonator has been printed

**Table 6**
*Comparison of MIMO Antenna Based on Parasitic Elements/Structures*

| References | Substrate area (l × b) $mm^2$, $\lambda_0 \times \lambda_0 = \lambda_0^2$ | Min. isolation (dB) | Max. ECC value and computation approach | Type of parasitic elements/structures | No. of elements | Narrowband/ wideband/ UWB |
|---|---|---|---|---|---|---|
| Kumar et al. (2018b) | 30 × 50, 0.31 × 0.51 = 0.16 | 16 | 0.01, *S*-parameters | Modified interdigital capacitor | 2 | UWB |
| Kumar et al. (2019a) | 56 × 70, 0.42 × 0.52 = 0.22 | 24 | 0.036, far-field | A novel ITI-shaped parasitic structure | 2 | Wideband (multiband) |
| Arun et al. (2014) | —, — | 34 | ~0, *S*-parameters | Modified serpentine structure | 2 | Narrowband |
| Singhal (2019) | 27 × 27, 0.43 × 0.43 = 0.18 | 15 | 0.005, *S*-parameters | Rotated "+" shaped rectangular strip pair | 4 | UWB |
| Faraz et al. (2019) | 30 × 80, 0.58 × 1.55 = 0.90 | 15 | —, — | Two separate rectangular shape and T-shaped parasitic elements | 4 | Narrowband |
| Alsath et al. (2013) | 54 × 45, 0.86 × 0.72 = 0.62 | 16 | —, — | Slotted meander-line resonator (SMLR) | 2 | Narrowband |
| Debnath et al. (2018) | 46 × 46, 0.48 × 0.48 = 0.23 | 17 | 0.02, *S*-parameters | Minkowski fractal-shaped isolators | 2 | UWB |
| Li et al. (2012) | 95 × 60, 0.61 × 0.38 = 0.23 | 20 | —, — | Two parasitic monopole | 2 | Narrowband |
| Liu et al. (2018) | 36 × 35, 0.23 × 0.22 = 0.05 | 15.4 | 0.14, far-field | Novel H-shaped parasitic element | 2 | Wideband |
| Mak et al. (2008) | 40 × 20, 0.32 × 0.16 = 0.05 | 30 | —, — | A T-shaped coupling element | 2 | Narrowband |
| Alsultan and Ögücü Yetkin (2018) | 41 × 100, 0.68 × 1.67 = 1.14 | 18 | 0.0001, *S*-parameters | 2 × 3 matrix of C-shaped resonator | 2 | Wideband |
| Wang et al. (2016) | 50 × 50, 0.41 × 0.41 = 0.17 | 16 | ~0, *S*-parameters | Parasitic fragment-type isolation element | 2 | Narrowband |
| Wen and Xin-Liang (2018) | 25 × 40, 0.42 × 0.67 = 0.28 | 36 | 0.0006, *S*-parameters | Periodic paperclip-shaped structure | 2 | Narrowband |

on the PCB between the two inverted-F antenna (IFA) (Wu et al., 2017), an additional folded resonator having an electrical length of half guided wavelength has been placed above connecting shorted metallic strip between two PIFA (Lee et al., 2009), and optimally designed resistor-loaded paired parallel-coupled resonators (PCRs) (Park et al., 2019), an I-shaped $\lambda/2$ resonator between microstrip array (Ghosh & Parui, 2014), dumbbell-shaped resonator between dual-trace dual-column coaxial microstrip array (Zhu et al., 2016), inverted U-shaped resonator and line resonator (Ghosh, 2016) and dual-band strip resonator as a wave trap (Kang & Wong, 2010) have been used to suppress the MC.

From the data in Table 6, the parasitic elements/structures help achieve high isolation for all the cases: narrowband; wideband; UWB; with an ultracompactness of $0.05\lambda_0^2$ (Mak et al., 2008; Liu et al., 2018). This approach is the most popular and straightforward to implement among so far discussed in the existing literature.

## 4. Conclusions and Future Scope

In all the above cases, it has been found that the isolation or suppressing of MC is a significant problem in the lower frequency range as the $\lambda$ increases with the decrease of the frequency. Also, the impact of MC increases as the distance between the two microstrip antennas becomes much lesser than $\lambda_0/2$. The more the antenna is compact, the less will be the distance between the microstrip antennas. Hence, it will deteriorate the MIMO antenna's performance, especially at a lower frequency: consequently, more concern should be considered at a lower frequency. ECC is the most crucial diversity parameter when discussing spatial/pattern diversity if computed with far-field radiation patterns. We find relatively higher values but <0.5 compared to the *S*-parameters approach of calculating ECC, which is generally significantly lower than 0.05 and focused mainly on port isolation. Protruding ground stubs, DGSs, slots/slits-etching, and parasitic elements/structures are widely suitable for reducing MC in wideband and UWB-MIMO antennas.

**Acknowledgment**
The authors acknowledge the CRS project having Application ID: 1-5748389248 sanctioned under TEQIP-III by the National Project Implementation Unit (NPIU), a unit of the Ministry of Human Resource Development (MHRD), Government of India.

## References

Abbosh, A. M. (2007). Analytical close-form solutions for different configurations of parallel-coupled microstrip lines. *IET Microwaves, Antennas & Propagation*, 561–566. https://doi.org/10.1049/iet-map

Abdalla, M. A., & Ibrahim, A. A. (2013). Compact and closely spaced metamaterial MIMO antenna with high isolation for wireless applications. *IEEE Antennas and Wireless Propagation Letters*, *12*, 1452–1455. https://doi.org/10.1109/LAWP.2013.2288338

Abid, M., Rehman, U., Ali, S., Iqbal, A., & Hameed, M. (2018). Design and analysis of UWB-MIMO antenna with enhanced isolation design and analysis of UWB-MIMO antenna with enhanced isolation. Paper presented at *3rd International Electrical Engineering Conference (IEEC 2018)* (pp. 1–4). Karachi, Pakistan: IEP Centre. Retrieved from http://ieec.neduet.edu.pk/2018/Papers_2018/11.pdf

Acharjee, J., Mandal, K., & Mandal, S. K. (2018). Reduction of mutual coupling and cross-polarization of a MIMO/diversity antenna using a string of H-shaped DGS. *AEU-International Journal of Electronics and Communications*, *97*, 110–119. https://doi.org/10.1016/j.aeue.2018.09.037

Addaci, R., Diallo, A., Luxey, C., Le Thuc, P., & Staraj, R. (2012). Dual-band WLAN diversity antenna system with high port-to-port isolation. *IEEE Antennas and Wireless Propagation Letters*, *11*, 244–247. https://doi.org/10.1109/LAWP.2012.2188824

Addaci, R., Haneda, K., Diallo, A., Le Thuc, P., Luxey, C., Staraj, R., & Vainikainen, P. (2014). Dual-band WLAN multiantenna system and diversity/MIMO performance evaluation. *IEEE Transactions on Antennas and Propagation*, *62*(3), 1409–1415. https://doi.org/10.1109/TAP.2013.2294955

Alsultan, R. G. S., & Ögücü Yetkin, G. (2018). Mutual coupling reduction of E-shaped MIMO antenna with matrix of C-shaped resonators. *International Journal of Antennas and Propagation*, *2018*, 4814176. https://doi.org/10.1155/2018/4814176

Aminu-Baba, M., Rahim, M. K. A., Zubir, F., Iliyasu, A. Y., Mohd Yusoff, M. F., Jahun, K. I., & Ayop, O. (2019). Compact patch MIMO antenna with low mutual coupling for WLAN applications. *ELEKTRIKA-Journal of Electrical Engineering*, *18*(1), 43–46. https://doi.org/10.11113/elektrika.v18n1.146

Anitha, R., Sarin, V. P., Mohanan, P., & Vasudevan, K. (2014). Enhanced isolation with defected ground structure in MIMO antenna. *Electronics Letters*, *50*(24), 1784–1786. https://doi.org/10.1049/el.2014.2795

Arun, H., Sarma, A. K., Kanagasabai, M., Velan, S., Raviteja, C., & Alsath, M. G. N. (2014). Deployment of modified serpentine structure for mutual coupling reduction in MIMO antennas. *IEEE Antennas and Wireless Propagation Letters*, *13*, 277–280. https://doi.org/10.1109/LAWP.2014.2304541

Asghar, T., Ijaz, B., Alimgeer, K. S., Khan, M. S., & Shubair, R. (2018). A compact UWB MIMO antenna with inverted U-shaped slot for WLAN rejection. Paper presented at *IEEE International Symposium on Personal, Indoor and Mobile Radio Communications* (pp. 1–4). PIMRC. https://doi.org/10.1109/PIMRC.2017.8292726

Ayatollahi, M., Rao, Q., & Wang, D. (2012). A compact, high isolation and wide bandwidth antenna array for long term evolution wireless devices. *IEEE Transactions on Antennas and Propagation*, *60*(10), 4960–4963. https://doi.org/10.1109/TAP.2012.2207312

Azarm, B., Nourinia, J., Ghobadi, C., Majidzadeh, M., & Hatami, N. (2019). On development of a MIMO antenna for coupling reduction and WiMAX suppression purposes. *AEU-International Journal of Electronics and Communications*, *99*, 226–235. https://doi.org/10.1016/j.aeue.2018.11.038

Ban, Y. L., Chen, Z. Z. X., Chen, Z. Z. X., Kang, K., & Li, J. L. W. (2014). Decoupled hepta-band antenna array for WWAN/LTE smartphone applications. *IEEE Antennas and Wireless Propagation Letters*, *13*, 999–1002. https://doi.org/10.1109/LAWP.2014.2325877

Bhanumathi, V., & Sivaranjani, G. (2019). High isolation MIMO antenna using semi-CIRCLE patch for UWB applications. *Progress in Electromagnetics Research C*, *92*, 31–40. https://doi.org/10.2528/PIERC19011805

Bhattacharya, A., Roy, B., Chowdhury, S. K., & Bhattacharjee, A. K. (2019). An isolation enhanced, printed, low-profile UWB-MIMO antenna with unique dual band-notching features for WLAN and WiMAX. *IETE Journal of Research*, 1–8. https://doi.org/10.1080/03772063.2019.1612284

Biswal, S. P., & Das, S. (2018a). A low-profile dual port UWB-MIMO/diversity antenna with band rejection ability. *International Journal of RF and Microwave Computer-Aided Engineering*, *28*(1), e21159. https://doi.org/10.1002/mmce.21159

Biswal, S. P., & Das, S. (2018b). Two-element printed PIFA-MIMO antenna system for WiMAX and WLAN applications. *IET Microwaves, Antennas and Propagation*, *12*(14), 2262–2270. https://doi.org/10.1049/iet-map.2018.5271

Biswal, S. P., & Das, S. (2019). A compact printed ultra-wideband multiple-input multiple-output prototype with band-notch ability for WiMAX, LTEband43, and WLAN systems. *International Journal of RF and Microwave Computer-Aided Engineering*, *29*(6), e21673. https://doi.org/10.1002/mmce.21673

Breed, B. G. (2008). An introduction to defected ground structures in microstrip circuits. *High Frequency Electronics*, *7*, 50–54.

Caizzone, S. (2017). Miniaturized E5a/E1 antenna array for robust GNSS navigation. *IEEE Antennas and Wireless Propagation Letters*, *16*, 485–488. https://doi.org/10.1109/LAWP.2016.2585353

Chacko, B. P., Augustin, G., & Denidni, T. A. (2013). Uniplanar polarisation diversity antenna for ultrawideband systems. *IET Microwaves, Antennas and Propagation*, *7*(10), 851–857. https://doi.org/10.1049/iet-map.2012.0732

Chandel, R., & Gautam, A. K. (2016). Compact MIMO/diversity slot antenna for UWB applications with band-notched characteristic. *Electronics Letters*, *52*(5), 336–338. https://doi.org/10.1049/el.2015.3889

Chandel, R., Gautam, A. K., & Rambabu, K. (2018). Tapered fed compact UWB MIMO-diversity antenna with dual band-notched characteristics. *IEEE Transactions on Antennas and Propagation*, *66*(4), 1677–1684. https://doi.org/10.1109/TAP.2018.2803134

Chen, X. (2015). Antenna correlation and its impact on multi-antenna system. *Progress in Electromagnetics Research B*, *62*(1), 241–253. https://doi.org/10.2528/PIERB15012805

Chen, Y. S., & Chang, C. P. (2016). Design of a four-element multiple-input-multiple-output antenna for compact long-term evolution small-cell base stations. *IET Microwaves, Antennas and Propagation*, *10*(4), 385–392. https://doi.org/10.1049/iet-map.2015.0540

Chiu, C.-Y., Cheng, C.-H., Murch, R. D., & Rowell, C. R. (2007). Reduction of mutual coupling between closely-packed antenna elements. *IEEE Transactions on Antennas and Propagation*, *55*(6), 1732–1738. https://doi.org/10.1109/TAP.2007.898618

Chouhan, S., Panda, D. K., Gupta, M., & Singhal, S. (2018). Multiport MIMO antennas with mutual coupling reduction techniques for modern wireless transreceive operations: A review. *International Journal of RF and Microwave Computer-Aided Engineering*, *28*(2), e21189. https://doi.org/10.1002/mmce.21189

Chouhan, S., Panda, D. K., & Kushwah, V. S. (2019). Modified circular common element four-port multiple-input-multiple-output antenna using diagonal parasitic element. *International Journal of RF and Microwave Computer-Aided Engineering*, *29*(2), e21527. https://doi.org/10.1002/mmce.21527

Chu, S., Hasan, M. N., Yan, J., & Chu, C. C. (2018). Tri-band $2\times 2$ 5G MIMO antenna array. Paper presented at *2018 Asia-Pacific Microwave Conference (APMC)* (pp. 1543–1545). IEEE. https://doi.org/10.23919/APMC.2018.8617590

Chung, K. L., & Kharkovsky, S. (2013). Mutual coupling reduction and gain enhancement using angular offset elements in circularly polarized patch array. *IEEE Antennas and Wireless Propagation Letters*, *12*, 1122–1124. https://doi.org/10.1109/LAWP.2013.2280656

Dama, Y. A. S., Abd-Alhameed, R. A., Jones, S. M. R., Zhou, D., McEwan, N. J., Child, M. B., & Excell, P. S. (2011). An envelope correlation formula for (N,N) MIMO antenna arrays using input scattering parameters, and including power losses. *International Journal of Antennas and Propagation*, *2011*, 421691. https://doi.org/10.1155/2011/421691

Debnath, P., Karmakar, A., Saha, A., & Huda, S. (2018). UMB MIMO Slot antenna with Minkowski fractal shaped isolators for isolation enhancement. *Progress in Electromagnetics Research*, *75*, 69–78. https://doi.org/10.2528/PIERM18090506

Deng, J., Li, J., Zhao, L., & Guo, L. (2017). A dual-band inverted-F MIMO antenna with enhanced isolation for WLAN applications. *IEEE Antennas and Wireless Propagation Letters*, *16*, 2270–2273. https://doi.org/10.1109/LAWP.2017.2713986

Dhar, S. K., & Sharawi, M. S. (2014). A multi-band isolation enhanced loaded semi-ring MIMO antenna. *European Microwave Week 2014: Connecting the Future, EuMW 2014-Conference Proceedings; EuMC 2014: 44th European Microwave Conference* (pp. 386–389). https://doi.org/10.1109/EuMC.2014.6986451

Dong, J., Wang, S., & Mo, J. (2020). Design of a twelve-port MIMO antenna system for multi-mode 4G/5G smartphone applications based on characteristic mode analysis. *IEEE Access*, *8*, 90751–90759. https://doi.org/10.1109/ACCESS.2020.2994068

Elsheakh, D. N., Elsadek, H. A., Abdallah, E. A., Iskander, M. F., & Elhenawy, H. (2010). Low mutual coupling $2 \times 2$ microstrip patch array antenna by using novel shapes of defect ground structure. *Microwave and Optical Technology Letters*, *52*(5), 1208–1215. https://doi.org/10.1002/mop.25152

Faraz, F., Li, Q., Chen, X., Abdullah, M., Zhang, S., & Zhang, A. (2019). Mutual coupling reduction for linearly arranged MIMO antenna. Paper presented at *2019 Cross Strait Quad-Regional Radio Science and Wireless Technology Conference. CSQRWC 2019-Proceedings* (pp. 1–3). https://doi.org/10.1109/CSQRWC.2019.8799266

Fritz-Andrade, E., Perez-Miguel, A., Gomez-Villanueva, R., & Jardon-Aguilar, H. (2020). Characteristic mode analysis applied to reduce the mutual coupling of a four-element patch MIMO antenna using a defected ground structure. *IET Microwaves, Antennas and Propagation*, *14*(2), 215–226. https://doi.org/10.1049/iet-map.2019.0570

Gangwar, D., Sharma, A., Kanaujia, B. K., Singh, S. P., & Lay-Ekuakille, A. (2020). Characterization and performance measurement of low RCS wideband circularly polarized MIMO antenna for microwave sensing applications. *IEEE Transactions on Instrumentation and Measurement*, *69*(6), 3847–3854. https://doi.org/10.1109/TIM.2019.2936707

Gao, D., Cao, Z. X., Fu, S. D., Quan, X., & Chen, P. (2020). A novel slot-array defected ground structure for decoupling microstrip antenna array. *IEEE Transactions on Antennas and Propagation*, *68*(10), 7027–7038. https://doi.org/10.1109/TAP.2020.2992881

Gao, P., He, S., Wei, X., Xu, Z., Wang, N., & Zheng, Y. (2014). Compact printed UWB diversity slot antenna with 5.5-GHz band-notched characteristics. *IEEE Antennas and Wireless Propagation Letters*, *13*, 376–379. https://doi.org/10.1109/LAWP.2014.2305772

Gautam, A. K., Saini, A., Agrawal, N., & Rizvi, N. Z. (2019). Design of a compact protrudent-shaped ultra-wideband multiple-input-multiple-output/diversity antenna with band-rejection capability. *International Journal of RF and Microwave Computer-Aided Engineering*, *29*(9), e21829. https://doi.org/10.1002/mmce.21829

Gautam, A. K., Yadav, S., & Rambabu, K. (2018). Design of ultra-compact UWB antenna with band-notched characteristics for MIMO applications. *IET Microwaves, Antennas and Propagation*, *12*(12), 1895–1900. https://doi.org/10.1049/iet-map.2018.0012

Ghimire, J., Choi, K.-W., & Choi, D.-Y. (2019). Bandwidth enhancement and mutual coupling reduction using a notch and a parasitic structure in a UWB-MIMO antenna. *International Journal of Antennas and Propagation*, *2019*, 8945386. https://doi.org/10.1155/2019/8945386

Ghosh, C. K. (2016). A compact 4-channel microstrip MIMO antenna with reduced mutual coupling. *AEU-International Journal of Electronics and Communications*, *70*(7), 873–879. https://doi.org/10.1016/j.aeue.2016.03.018

Ghosh, C. K., & Parui, S. K. (2014). Elimination of scan blindness of microstrip array by using I-shaped λ/2 resonator. *Microwave and Optical Technology Letters*, *56*(2), 334–338. https://doi.org/10.1002/mop.28094

Ghouz, H. H. M. (2015). Novel compact and dual-broadband microstrip MIMO antennas for wireless applications. *Progress in Electromagnetics Research B*, *63*(1), 107–121. https://doi.org/10.2528/PIERB15051304

Govindarajulu, S. R., Jenkel, A., Hokayem, R., & Alwan, E. A. (2020). Mutual coupling suppression in antenna arrays using meandered open stub filtering technique. *IEEE Open Journal of Antennas and Propagation*, *1*, 379–386. https://doi.org/10.1109/OJAP.2020.3010153

Gulam Nabi Alsath, M., Kanagasabai, M., & Balasubramanian, B. (2013). Implementation of slotted meander-line resonators for isolation enhancement in microstrip patch antenna arrays. *IEEE Antennas and Wireless Propagation Letters*, *12*, 15–18. https://doi.org/10.1109/LAWP.2012.2237156

Habashi, A., Nourinia, J., & Ghobadi, C. (2011). Mutual coupling reduction between very closely spaced patch antennas using low-profile folded split-ring resonators (FSRRs). *IEEE Antennas and Wireless Propagation Letters*, *10*, 862–865. https://doi.org/10.1109/LAWP.2011.2165931

Hatami, N., Nourinia, J., Ghobadi, C., Majidzadeh, M., & Azarm, B. (2019). High inter-element isolation and WLAN filtering mechanism: A compact MIMO antenna scheme. *AEU-International Journal of Electronics and Communications*, *109*, 43–54. https://doi.org/10.1016/j.aeue.2019.07.001

Hong, S., Chung, K., Lee, J., Jung, S., Lee, S. S., & Choi, J. (2008). Design of a diversity antenna with stubs for UWB applications. *Microwave and Optical Technology Letters*, *50*(5), 1352–1356. https://doi.org/10.1002/mop.23389

Huang, H., Liu, Y., & Gong, S. X. (2015a). Four antenna MIMO system with compact radiator for mobile terminals. *Microwave and Optical Technology Letters*, *57*(6), 1281–1286. https://doi.org/10.1002/mop.29074

Huang, H., Liu, Y., Zhang, S.-S., & Gong, S.-X. (2015b). Compact polarization diversity ultrawideband MIMO antenna with triple band-notched characteristics. *Microwave and Optical Technology Letters*, *57*(4), 946–953. https://doi.org/10.1002/mop.28957

Huang, H. F., & Xiao, S. G. (2015). Compact triple band-notched UWB MIMO antenna with simple stepped stub to enhance wideband isolation. *Progress in Electromagnetics Research Letters*, *56*, 59–65. https://doi.org/10.2528/PIERL15081405

Hussain, R., Khan, M. U., & Sharawi, M. S. (2018). An integrated dual MIMO antenna system with dual-function GND-plane frequency-Agile antenna. *IEEE Antennas and Wireless Propagation Letters*, *17*(1), 142–145. https://doi.org/10.1109/LAWP.2017.2778182

Hussain, R., Raza, A., Khan, M. U., Shammim, A., & Sharawi, M. S. (2019). Miniaturized frequency reconfigurable pentagonal MIMO slot antenna for interweave CR applications. *International Journal of RF and Microwave Computer-Aided Engineering*, *29*(9), e21811. https://doi.org/10.1002/mmce.21811

Hwang, S. H., Yang, T. S., Byun, J. H., & Kim, A. S. (2010). Complementary pattern method to reduce mutual coupling in metamaterial antennas. *IET Microwaves, Antennas and Propagation*, *4*(9), 1397–1405. https://doi.org/10.1049/iet-map.2008.0373

Ikram, M., Sharawi, M. S., Shamim, A., & Sebak, A. (2018). A multiband dual-standard MIMO antenna system based on monopoles (4G) and connected slots (5G) for future smart phones. *Microwave and Optical Technology Letters*, *60*(6), 1468–1476. https://doi.org/10.1002/mop.31180

Iqbal, A., Saraereh, O. A., Ahmad, A. W., & Bashir, S. (2017). Mutual coupling reduction using F-shaped stubs in UWB-MIMO antenna. *IEEE Access*, *6*, 2755–2759. https://doi.org/10.1109/ACCESS.2017.2785232

Irene, G., & Rajesh, A. (2018a). Review on the design of the isolation techniques for UWB-MIMO antennas. *Advanced Electromagnetics*, *7*(4), 46–70. https://doi.org/10.7716/AEM.V7I4.743

Irene, G., & Rajesh, A. (2018b). A penta-band reject inside cut Koch fractal hexagonal monopole UWB MIMO antenna for portable devices. *Progress in Electromagnetics Research C*, *82*, 225–235. https://doi.org/10.2528/pierc18020604

Isaac, A. A., Al-Rizzo, H., Yahya, S., Al-Wahhamy, A., & Abushamleh, S. (2018). Decoupling of two closely-spaced planar monopole antennas using two novel printed-circuit structures. *Microwave and Optical Technology Letters*, *60*(12), 2954–2963. https://doi.org/10.1002/mop.31405

Jaglan, N., Gupta, S. D., Thakur, E., Kumar, D., Kanaujia, B. K., & Srivastava, S. (2018). Triple band notched mushroom and uniplanar EBG structures based UWB MIMO/diversity antenna with enhanced wide band isolation. *AEU-International Journal of Electronics and Communications*, *90*, 36–44. https://doi.org/10.1016/j.aeue.2018.04.009

Jaglan, N., Kanaujia, B. K., Gupta, S. D., & Srivastava, S. (2017). Dual band notched EBG structure based UWB MIMO/diversity antenna with reduced wide band electromagnetic coupling. *Frequenz*, *71*(11–12), 555–565. https://doi.org/10.1515/freq-2016-0325

Jamal, M. Y., Li, M., & Yeung, K. L. (2020). Isolation enhancement of closely packed dual circularly polarized MIMO antenna using hybrid technique. *IEEE Access*, *8*, 11241–11247. https://doi.org/10.1109/ACCESS.2020.2964902

Jetti, C. R., & Nandanavanam, V. R. (2018). Trident-shape strip loaded dual band-notched UWB MIMO antenna for portable device applications. *AEU-International Journal of Electronics and Communications*, *83*, 11–21. https://doi.org/10.1016/j.aeue.2017.08.021

Kang, L., Li, H., Wang, X., & Shi, X. (2015). Compact offset microstrip-fed MIMO antenna for band-notched UWB applications. *IEEE Antennas and Wireless Propagation Letters*, *14*, 1754–1757. https://doi.org/10.1109/LAWP.2015.2422571

Kang, L., Li, H., Wang, X. H., & Shi, X. W. (2016). Miniaturized band-notched UWB MIMO antenna with high isolation. *Microwave and Optical Technology Letters*, *58*(4), 878–881. https://doi.org/10.1002/mop.29691

Kang, T.-W., & Wong, K.-L. (2010). Isolation improvement of 2.4/5.2/5.8 GHz WLAN internal laptop computer antennas using dual-band strip resonator as a wavetrap. *Microwave and Optical Technology Letters*, *52*(1), 58–64. https://doi.org/10.1002/mop.24831

Karimian, R., Soleimani, M., & Hashemi, S. M. (2012). Tri-band four elements MIMO antenna system for WLAN and WiMAX application. *Journal of Electromagnetic Waves and Applications*, *26*(17–18), 2348–2357. https://doi.org/10.1080/09205071.2012.734433

Khan, M. S., Capobianco, A.-D., Asif, S. M., Anagnostou, D. E., Shubair, R. M., & Braaten, B. D. (2017a). A compact CSRR-enabled UWB diversity antenna. *IEEE Antennas and Wireless Propagation Letters*, *16*, 808–812. https://doi.org/10.1109/LAWP.2016.2604843

Khan, M. S., Capobianco, A. D., Iftikhar, A., Shubair, R. M., Anagnostou, D. E., & Braaten, B. D. (2017b). Ultra-compact dual-polarised UWB MIMO antenna with meandered feeding lines. *IET Microwaves, Antennas and Propagation*, *11*(7), 997–1002. https://doi.org/10.1049/iet-map.2016.1074

Khan, M. S., Capobianco, A. D., Najam, A. I., Shoaib, I., Autizi, E., & Shafique, M. F. (2014). Compact ultra-wideband diversity antenna with a floating parasitic digitated decoupling structure. *IET Microwaves, Antennas and Propagation*, *8*(10), 747–753. https://doi.org/10.1049/iet-map.2013.0672

Khan, M. S., Iftikhar, A., Shubair, R. M., Capobianco, A.-D., Braaten, B. D., & Anagnostou, D. E. (2020). Eight-element compact UWB-MIMO/Diversity antenna with WLAN band rejection for 3G/4G/5G communications. *IEEE Open Journal of Antennas and Propagation*, *1*, 196–206. https://doi.org/10.1109/OJAP.2020.2991522

Khan, M. S., Shafique, M. F., Naqvi, A., Capobianco, A.-D., Ijaz, B., & Braaten, B. D. (2015). A miniaturized dual-band MIMO antenna for WLAN applications. *IEEE Antennas and Wireless Propagation Letters*, *14*, 958–961. https://doi.org/10.1109/LAWP.2014.2387701

Khandelwal, M. K., Kanaujia, B. K., & Kumar, S. (2017). Defected ground structure: Fundamentals, analysis, and applications in modern wireless trends. *International Journal of Antennas and Propagation*, *2017*, 2018527. https://doi.org/10.1155/2017/2018527

Kim, I., Jung, C. W., Kim, Y., & Kim, Y. E. (2008). Low-profile wideband MIMO antenna with suppressing mutual coupling between two antennas. *Microwave and Optical Technology Letters*, *50*(5), 1336–1339. https://doi.org/10.1002/mop.23368

Krishna, R. V. S. R., & Kumar, R. (2016). A dual-polarized square-ring slot antenna for UWB, imaging, and radar applications. *IEEE Antennas and Wireless Propagation Letters*, *15*, 195–198. https://doi.org/10.1109/LAWP.2015.2438013

Kumar, A., Ansari, A. Q., Kanaujia, B. K., & Kishor, J. (2018a). High isolation compact four-port MIMO antenna loaded with CSRR for multiband applications. *Frequenz*, *72*(9–10), 415–427. https://doi.org/10.1515/freq-2017-0276

Kumar, A., Ansari, A. Q., Kanaujia, B. K., & Kishor, J. (2019a). A novel ITI-shaped isolation structure placed between two-port CPW-fed dual-band MIMO antenna for high isolation. *AEU-International Journal of Electronics and Communications*, *104*, 35–43. https://doi.org/10.1016/j.aeue.2019.03.009

Kumar, A., Ansari, A. Q., Kanaujia, B. K., & Kishor, J. (2019b). Dual circular polarization with reduced mutual coupling among two orthogonally placed CPW-fed microstrip antennas for broadband Applications. *Wireless Personal Communications*, *107*(2), 759–770. https://doi.org/10.1007/s11277-019-06298-x

Kumar, A., Ansari, A. Q., Kanaujia, B. K., Kishor, J., & Kumar, S. (2020a). An ultra-compact two-port UWB-MIMO antenna with dual band-notched characteristics. *AEU-International Journal of Electronics and Communications*, *114*, 152997. https://doi.org/10.1016/j.aeue.2019.152997

Kumar, A., Ansari, A. Q., Kanaujia, B. K., Kishor, J., & Tewari, N. (2018b). Design of triple-band MIMO antenna with one band-notched characteristic. *Progress in Electromagnetics Research C*, *86*, 41–53. https://doi.org/10.2528/PIERC18051902

Kumar, A., & Kartikeyan, M. V. (2020b). Design and studies of bandstop filters using modified CSRR DGS for WLAN applications. In V. Janyani, G. Singh, M. Tiwari, & A. D'Alessandro (Eds.), *Optical and wireless technologies. Lecture notes in electrical engineering* (Vol. *546*, pp. 467–475). Singapore: Springer. https://doi.org/10.1007/978-981-13-6159-3_49

Kumar, S., Kumar, R., Kumar Vishwakarma, R., & Srivastava, K. (2018c). An improved compact MIMO antenna for wireless applications with band-notched characteristics. *AEU-International Journal of Electronics and Communications*, *90*, 20–29. https://doi.org/10.1016/j.aeue.2018.04.008

Kumar, P., Urooj, S., & Alrowais, F. (2020c). Design and implementation of quad-port MIMO antenna with dual-band elimination characteristics for ultra-wideband applications. *Applied Sciences*, *10*(5), 1715. https://doi.org/10.3390/app10051715

Kumar, P., Urooj, S., & Malibari, A. (2020d). Design of quad-port ultra-wideband multiple-input-multiple-output antenna with wide axial-ratio bandwidth. *Sensors*, *20*(4), 1174. https://doi.org/10.3390/s20041174

Lee, C. H., Chen, S. Y., & Hsu, P. (2009). Integrated dual planar inverted-F antenna with enhanced isolation. *IEEE Antennas and Wireless Propagation Letters*, *8*, 963–965. https://doi.org/10.1109/LAWP.2009.2029707

Lee, J. M., Kim, K. B., Ryu, H. K., & Woo, J. M. (2012). A compact ultrawideband MIMO antenna with WLAN band-rejected operation for mobile devices. *IEEE Antennas and Wireless Propagation Letters*, *11*, 990–993. https://doi.org/10.1109/LAWP.2012.2214431

Li, H., Xiong, J., & He, S. (2009). A compact planar MIMO antenna system of four elements with similar radiation characteristics and isolation structure. *IEEE Antennas and Wireless Propagation Letters*, *8*, 1107–1110. https://doi.org/10.1109/LAWP.2009.2034110

Li, J. F., Chu, Q. X., Li, Z. H., & Xia, X. X. (2013a). Compact dual band-notched UWB MIMO antenna with high isolation. *IEEE Transactions on Antennas and Propagation*, *61*(9), 4759–4766. https://doi.org/10.1109/TAP.2013.2267653

Li, Q., Ding, C., Yang, R., Tan, M., Wu, G., Lei, X., et al. (2018). Mutual coupling reduction between patch antennas using meander line. *International Journal of Antennas and Propagation*, *2018*, 2586382. https://doi.org/10.1155/2018/2586382

Li, W. T., Hei, Y. Q., Subbaraman, H., Shi, X. W., & Chen, R. T. (2016). Novel printed filtenna with dual notches and good out-of-band characteristics for UWB-MIMO applications. *IEEE Microwave and Wireless Components Letters*, *26*(10), 765–767. https://doi.org/10.1109/LMWC.2016.2601298

Li, Y., Li, W., & Yu, W. (2013b). A multi-band/UWB MIMO/diversity antenna with an enhanced isolation using radial stub loaded resonator. *Applied Computational Electromagnetics Society Journal*, *28*(1), 8–20.

Li, Z., Du, Z., Takahashi, M., Saito, K., & Ito, K. (2012). Reducing mutual coupling of MIMO antennas with parasitic elements for mobile terminals. *IEEE Transactions on Antennas and Propagation*, *60*(2), 473–481. https://doi.org/10.1109/TAP.2011.2173432

Li, Z., Yin, C., & Zhu, X. (2019). Compact UWB MIMO Vivaldi antenna with dual band-notched characteristics. *IEEE Access*, *7*, 38696–38701. https://doi.org/10.1109/ACCESS.2019.2906338

Liao, W.-J., Hsieh, C.-Y., Dai, B.-Y., & Hsiao, B.-R. (2015). Inverted-F/slot integrated dual-band four-antenna system for WLAN access points. *IEEE Antennas and Wireless Propagation Letters*, *14*, 847–850. https://doi.org/10.1109/LAWP.2014.2381362

Liu, L., Cheung, S. W., & Yuk, T. I. (2013). Compact MIMO antenna for portable devices in UWB applications. *IEEE Transactions on Antennas and Propagation*, *61*(8), 4257–4264. https://doi.org/10.1109/TAP.2013.2263277

Liu, L., Cheung, S. W., & Yuk, T. I. (2015). Compact MIMO antenna for portable UWB applications with band-notched characteristic. *IEEE Transactions on Antennas and Propagation*, *63*(5), 1917–1924. https://doi.org/10.1109/TAP.2015.2406892

Liu, X., Amin, M., & Liang, J. (2018). Wideband MIMO antenna with enhanced isolation for wireless communication application. *IEICE Electronics Express*, *15*(22), 245–252. https://doi.org/10.1587/elex.15.20180948

Lu, J., Kuai, Z., Zhu, X., & Zhang, N. (2011). A high-isolation dual-polarization microstrip patch antenna with quasi-cross-shaped coupling slot. *IEEE Transactions on Antennas and Propagation*, *59*(7), 2713–2717. https://doi.org/10.1109/TAP.2011.2152333

Lu, D., Wang, L., Yang, E., & Wang, G. (2018). Design of high-isolation wideband dual-polarized compact MIMO antennas with multi-objective optimization. *IEEE Transactions on Antennas and Propagation*, *66*(3), 1522–1527. https://doi.org/10.1109/TAP.2017.2784446

Luo, Y., Chu, Q. X., Li, J. F., & Wu, Y. T. (2013). A planar H-shaped directive antenna and its application in compact MIMO antenna. *IEEE Transactions on Antennas and Propagation*, *61*(9), 4810–4814. https://doi.org/10.1109/TAP.2013.2267193

Mak, A. C. K., Rowell, C. R., & Murch, R. D. (2008). Isolation enhancement between two closely packed antennas. *IEEE Transactions on Antennas and Propagation*, *56*(11), 3411–3419. https://doi.org/10.1109/TAP.2008.2005460

Malviya, L., Panigrahi, R. K., & Kartikeyan, M. V. (2016a). 2 × 2 MIMO antenna for ISM band application. Paper presented at *2016 11th International Conference on Industrial and Information Systems (ICIIS)* (pp. 794–797). IEEE. https://doi.org/10.1109/ICIINFS.2016.8263047

Malviya, L., Panigrahi, R. K., & Kartikeyan, M. V. (2016b). A 2 × 2 dual-band MIMO antenna with polarization diversity for wireless applications. *Progress in Electromagnetics Research C*, *61*, 91–103. https://doi.org/10.2528/PIERC15110401

Malviya, L., Panigrahi, R. K., & Kartikeyan, M. V. (2017). MIMO antennas with diversity and mutual coupling reduction techniques: A review. *International Journal of Microwave and Wireless Technologies*, *9*(8), 1763–1780. https://doi.org/10.1017/S1759078717000538

Mao, C. X., & Chu, Q. X. (2014). Compact coradiator UWB-MIMO antenna with dual polarization. *IEEE Transactions on Antennas and Propagation*, *62*(9), 4474–4480. https://doi.org/10.1109/TAP.2014.2333066

Marzudi, W. N. N. W., Abidin, Z. Z., Dahlan, S. H., Yue, M., Abd-Alhameed, R. A., & Child, M. B. (2015). A compact orthogonal wideband printed MIMO antenna for WiFi/WLAN/LTE applications. *Microwave and Optical Technology Letters*, *57*(7), 1733–1738. https://doi.org/10.1002/mop.29140

Mathur, R., & Dwari, S. (2018a). Compact 4-Port UWB-MIMO slot antenna with dual polarization and low correlation for spatial diversity application. *Frequenz*, *72*(11–12), 503–509. https://doi.org/10.1515/freq-2018-0060

Mathur, R., & Dwari, S. (2018b). Compact CPW-Fed ultrawideband MIMO antenna using hexagonal ring monopole antenna elements. *AEU-International Journal of Electronics and Communications*, *93*, 1–6. https://doi.org/10.1016/j.aeue.2018.05.032

Mathur, R., & Dwari, S. (2019a). A compact UWB-MIMO with dual grounded CRR for isolation improvement. *International Journal of RF and Microwave Computer-Aided Engineering*, *29*(1), e21500. https://doi.org/10.1002/mmce.21500

Mathur, R., & Dwari, S. (2019b). Compact planar reconfigurable UWB-MIMO antenna with on-demand worldwide interoperability for microwave access/wireless local area network rejection. *IET Microwaves, Antennas & Propagation*, *13*(10), 1684–1689. https://doi.org/10.1049/iet-map.2018.6048

Mchbal, A., Amar Touhami, N., Elftouh, H., & Dkiouak, A. (2018). Mutual coupling reduction using a protruded ground branch structure in a compact UWB owl-shaped MIMO antenna. *International Journal of Antennas and Propagation*, *2018*, 4598527. https://doi.org/10.1155/2018/4598527

Min, K. S., Kim, D. J., & Moon, Y. M. (2005). Improved MIMO antenna by mutual coupling suppression between elements. Paper presented at *Wireless Technology 2005 Conference Proceedings-8th European Conference on Wireless Technology* (Vol. *2005*, pp. 135–138). https://doi.org/10.1109/ecwt.2005.1617671

Minz, L., & Garg, R. (2010). Reduction of mutual coupling between closely spaced PIFAs. *Electronics Letters*, *46*(6), 392–393. https://doi.org/10.1049/el.2010.3275

MoradiKordalivand, A., Rahman, T. A., & Khalily, M. (2014). Common elements wideband MIMO antenna system for WiFi/LTE access-point applications. *IEEE Antennas and Wireless Propagation Letters*, *13*, 1601–1604. https://doi.org/10.1109/LAWP.2014.2347897

Nadeem, I., & Choi, D.-Y. (2019). Study on mutual coupling reduction technique for MIMO antennas. *IEEE Access*, *7*, 563–586. https://doi.org/10.1109/ACCESS.2018.2885558

Nandi, S., & Mohan, A. (2017). A compact dual-band MIMO slot antenna for WLAN applications. *IEEE Antennas and Wireless Propagation Letters*, *16*, 2457–2460. https://doi.org/10.1109/LAWP.2017.2723927

Nie, L. Y., Lin, X. Q., Wang, B., & Zhang, J. (2019). A planar multifunctional four-port antenna system for sub-urban mobile tablet. *IEEE Access*, *7*, 56986–56993. https://doi.org/10.1109/ACCESS.2019.2913505

Nirdosh, Tan, C. M., & Tripathy, M. R. (2018). A miniaturized T-shaped MIMO antenna for X-band and Ku-band applications with enhanced radiation efficiency. Paper presented at *2018 27th Wireless and Optical Communication Conference (WOCC)* (Vol. 2018, pp. 1–5). https://doi.org/10.1109/WOCC.2018.8372695

Nirmal, P. C., Nandgaonkar, A., Nalbalwar, S., & Gupta, R. K. (2019). Compact wideband MIMO antenna for 4G WI-MAX, WLAN and UWB applications. *AEU-International Journal of Electronics and Communications*, *99*, 284–292. https://doi.org/10.1016/j.aeue.2018.12.008

Numan, A. B., Sharawi, M. S., Steffes, A., & Aloi, D. N. (2013). A defected ground structure for isolation enhancement in a printed MIMO antenna system. Paper presented at *2013 7th European Conference on Antennas and Propagation* (pp. 2123–2126). EuCAP 2013. Retrieved from https://ieeexplore.ieee.org/document/6546669

Ojaroudi, N., Ghadimi, N., Mehranpour, M., Ojaroudi, Y., & Ojaroudi, S. (2014). A new design of triple-band WLAN/WiMAX monopole antenna for multiple-input/multiple-output applications. *Microwave and Optical Technology Letters*, *56*(11), 2667–2671. https://doi.org/10.1002/mop.28675

Ouyang, J., Yang, F., & Wang, Z. M. (2011). Reducing mutual coupling of closely spaced microstrip MIMO antennas for WLAN application. *IEEE Antennas and Wireless Propagation Letters*, *10*, 310–313. https://doi.org/10.1109/LAWP.2011.2140310

Park, J., Choi, J., Park, J. Y., & Kim, Y. S. (2012). Study of a T-shaped slot with a capacitor for high isolation between MIMO antennas. *IEEE Antennas and Wireless Propagation Letters*, *11*, 1541–1544. https://doi.org/10.1109/LAWP.2012.2226695

Park, J. D., Rahman, M., & Chen, H. N. (2019). Isolation enhancement of wide-band MIMO array antennas utilizing resistive loading. *IEEE Access*, *7*, 81020–81026. https://doi.org/10.1109/ACCESS.2019.2923330

Paulraj, A. J., Gore, D. A., Nabar, R. U., & Bölcskei, H. (2004). An overview of MIMO communications—A key to gigabit wireless. *Proceedings of the IEEE*, *92*(2), 198–217. https://doi.org/10.1109/JPROC.2003.821915

Payandehjoo, K., & Abhari, R. (2014). Investigation of parasitic elements for coupling reduction in multiantenna hand-set devices. *International Journal of RF and Microwave Computer-Aided Engineering*, *24*(1), 1–10. https://doi.org/10.1002/mmce.20706

Ramachandran, A., Mathew, S., Viswanathan, V. P., Pezholil, M., & Kesavath, V. (2016). Diversity-based four-port multiple input multiple output antenna loaded with interdigital structure for high isolation. *IET Microwaves, Antennas and Propagation*, *10*(15), 1633–1642. https://doi.org/10.1049/iet-map.2015.0828

Rekha, V. S. D., Pardhasaradhi, P., Madhav, B. T. P., & Devi, Y. U. (2020). Dual band notched orthogonal 4-element MIMO antenna with isolation for UWB applications. *IEEE Access*, *8*, 145871–145880. https://doi.org/10.1109/ACCESS.2020.3015020

Ren, J., Hu, W., Yin, Y., & Fan, R. (2014). Compact printed MIMO antenna for UWB applications. *IEEE Antennas and Wireless Propagation Letters*, *13*, 1517–1520. https://doi.org/10.1109/LAWP.2014.2343454

Roshna, T. K., Deepak, U., Sajitha, V. R., Vasudevan, K., & Mohanan, P. (2015). A compact UWB MIMO antenna with reflector to enhance isolation. *IEEE Transactions on Antennas and Propagation*, *63*(4), 1873–1877. https://doi.org/10.1109/TAP.2015.2398455

Sarkar, D., & Srivastava, K. V. (2017). Compact four-element SRR-loaded dual-band MIMO antenna for WLAN/WiMAX/WiFi/4G-LTE and 5G applications. *Electronics Letters*, *53*(25), 1623–1624. https://doi.org/10.1049/el.2017.2825

Saxena, S., Kanaujia, B. K., Dwari, S., Kumar, S., & Tiwari, R. (2017). A compact dual-polarized MIMO antenna with distinct diversity performance for UWB applications. *IEEE Antennas and Wireless Propagation Letters*, *16*, 3096–3099. https://doi.org/10.1109/LAWP.2017.2762426

Sharawi, M. S. (2013). Printed MIMO antenna systems: Performance metrics, implementations and challenges. *Fermat*, *55*(1). https://doi.org/10.13140/2.1.1247.2966

Sharawi, M. S., Iqbal, S. S., & Faouri, Y. S. (2011). An 800 MHz 2 × 1 compact MIMO antenna system for LTE handsets. *IEEE Transactions on Antennas and Propagation*, *59*(8), 3128–3131. https://doi.org/10.1109/TAP.2011.2158958

Sharawi, M. S., Jan, M. A., & Aloi, D. N. (2012). Four-shaped 2 × 2 multi-standard compact multiple-input-multiple-output antenna system for long-term evolution mobile handsets. *IET Microwaves, Antennas and Propagation*, *6*(6), 685–696. https://doi.org/10.1049/iet-map.2011.0528

Sharawi, M. S., Podilchak, S. K., Khan, M. U., & Antar, Y. M. (2017). Dual-frequency DRA-based MIMO antenna system for wireless access points. *IET Microwaves, Antennas and Propagation*, *11*(8), 1174–1182. https://doi.org/10.1049/iet-map.2016.0671

Shoaib, S., Shoaib, I., Shoaib, N., Chen, X., & Parini, C. G. (2014). Design and performance study of a dual-element multiband printed monopole antenna array for MIMO terminals. *IEEE Antennas and Wireless Propagation Letters*, *13*, 329–332. https://doi.org/10.1109/LAWP.2014.2305798

Shoaib, S., Shoaib, I., Shoaib, N., Chen, X., & Parini, C. G. (2015). MIMO antennas for mobile handsets. *IEEE Antennas and Wireless Propagation Letters*, *14*, 799–802. https://doi.org/10.1109/LAWP.2014.2385593

Silveira, D., Gilabert Pinal, P., Lavrador, P., Pedro, J., Gadringer, M., Montoro López, G., et al. (2009). Improvements and analysis of nonlinear parallel behavioral models. *International Journal of RF and Microwave Computer-Aided Engineering*, *19*(5), 615–626. https://doi.org/10.1002/mmce

Singh, H. S., Meruva, B., Pandey, G. K., Bharti, P. K., & Meshram, M. K. (2013). Wire troubleshooting and diagnosis: Review and perspectives. *Progress in Electromagnetics Research B*, *53*,205–221. https://doi.org/10.2528/PIERB13020115

Singh, H. S., Pandey, G. K., Bharti, P. K., & Meshram, M. K. (2015). A compact dual-band diversity antenna for WLAN applications with high isolation. *Microwave and Optical Technology Letters*, *57*(4), 906–912. https://doi.org/10.1002/mop.28985

Singh, H. V., & Tripathi, S. (2019). Compact UWB MIMO antenna with cross-shaped unconnected ground stub using characteristic mode analysis. *Microwave and Optical Technology Letters*, *61*(7), 1874–1881. https://doi.org/10.1002/mop.31792

Singhal, S. (2019). Four element ultra-wideband fractal multiple-input multiple-output antenna. *Microwave and Optical Technology Letters*, *61*(12), 2811–2818. https://doi.org/10.1002/mop.31980

Sonkki, M., & Salonen, E. (2010). Low mutual coupling between monopole antennas by using two λ/2 slots. *IEEE Antennas and Wireless Propagation Letters*, *9*, 138–141. https://doi.org/10.1109/LAWP.2010.2044476

Srivastava, G., & Kanuijia, B. K. (2015). Compact dual band-notched UWB MIMO antenna with shared radiator. *Microwave and Optical Technology Letters*, *57*(12), 2886–2891. https://doi.org/10.1002/mop.29459

Srivastava, G., Kanuijia, B. K., & Paulus, R. (2016). UWB MIMO antenna with common radiator. *International Journal of Microwave and Wireless Technologies*, *9*(3), 573–580. https://doi.org/10.1017/S175907871500135X

Srivastava, G., & Mohan, A. (2015). Compact dual-polarized UWB diversity antenna. *Microwave and Optical Technology Letters*, *57*(12), 2951–2955. https://doi.org/10.1002/mop.29476

Srivastava, K., Kumar, A., Kanaujia, B. K., Dwari, S., & Kumar, S. (2019). A CPW-fed UWB MIMO antenna with integrated GSM band and dual band notches. *International Journal of RF and Microwave Computer-Aided Engineering*, *29*(1), e21433. https://doi.org/10.1002/mmce.21433

Stjernman, A. (2005). Relationship between radiation pattern correlation and scattering matrix of lossless and lossy antennas. *Electronics Letters*, *41*(12), 678–680. https://doi.org/10.1049/el:20050988

Tao, J., & Feng, Q. (2016). Compact UWB band-notch MIMO antenna with embedded antenna element for improved band notch filtering. *Progress in Electromagnetics Research C*, *67*, 117–125. https://doi.org/10.2528/PIERC16071903

Thummaluru, S. R., Ameen, M., & Chaudhary, R. K. (2019). Four-port MIMO cognitive radio system for midband 5G applications. *IEEE Transactions on Antennas and Propagation*, *67*(8), 5634–5645. https://doi.org/10.1109/TAP.2019.2918476

Thuwaini, A. H. R. (2018). *Mutual coupling suppression in multiple microstrip antennas for wireless applications (PhD dissertation)*. Brunel University London.

Toktas, A. (2017). G-shaped band-notched ultra-wideband MIMO antenna system for mobile terminals. *IET Microwaves, Antennas and Propagation*, *11*(5), 718–725. https://doi.org/10.1049/iet-map.2016.0820

Ul Haq, M. A., & Koziel, S. (2018). Ground plane alterations for design of high-isolation compact wideband MIMO antenna. *IEEE Access*, *6*, 48978–48983. https://doi.org/10.1109/ACCESS.2018.2867836

Usha Devi, Y., Madhav Tp, B., Anil Kumar, T., Sri Kavya, Ch. K., & Pardhasaradhi, P. (2020). Conformal printed MIMO antenna with DGS for millimetre wave communication applications. *International Journal of Electronics Letters*, *8*(3), 329–343. https://doi.org/10.1080/21681724.2019.1600731

Vasu Babu, K., & Anuradha, B. (2020). Design of nine-shaped MIMO antenna using parasitic elements to reduce mutual coupling. In *Lecture notes in electrical engineering* (pp. 31–37). Singapore: Springer. https://doi.org/10.1007/978-981-15-2926-9_4

Vaughan, R. G., & Andersen, J. B. (1987). Antenna diversity in mobile communications. *IEEE Transactions on Vehicular Technology*, *36*(4), 149–172. https://doi.org/10.1109/T-VT.1987.24115

Wang, F., Li, S., Zhou, Q., & Gong, Y. (2019). Compact wideband quad-element MIMO antenna with reversed S-shaped walls. *Progress in Electromagnetics Research M*, *78*, 193–201. https://doi.org/10.2528/PIERM19010201

Wang, H., Liu, L., Zhang, Z., Li, Y., & Feng, Z. (2015). A wideband compact WLAN/WiMAX MIMO antenna based on dipole with V-shaped ground branch. *IEEE Transactions on Antennas and Propagation*, *63*(5), 2290–2295. https://doi.org/10.1109/TAP.2015.2405091

Wang, L., Wang, G., & Sidén, J. (2014). Design of fragment-type isolation structures for MIMO antennas. *Progress in Electromagnetics Research C*, *52*, 71–82. https://doi.org/10.2528/PIERC14051504

Wang, L., Wang, G., & Zhao, Q. (2016). Suppressing mutual coupling of MIMO antennas with parasitic fragment-type elements. Paper presented at *2016 46th European Microwave Conference (EuMC)* (pp. 1303–1306). IEEE. https://doi.org/10.1109/EuMC.2016.7824590

Wang, W., Zhao, Z., Sun, Q., Liao, X., Fang, Z., See, K. Y., & Zheng, Y. (2020). Compact quad-element vertically-polarized high-isolation wideband MIMO antenna for vehicular base station. *IEEE Transactions on Vehicular Technology*, *69*(9), 10000–10008. https://doi.org/10.1109/tvt.2020.3004647

Wani, Z., & Vishwakarma, D. K. (2016). An ultrawideband antenna for portable MIMO terminals. *Microwave and Optical Technology Letters*, *58*(1), 51–56. https://doi.org/10.1002/mop.29498

Webster, J. G., Bhuiyan, M. S., & Karmakar, N. C. (2014). Defected ground structures for microwave applications. In J. G. Webster (Ed.), *Wiley encyclopaedia of electrical and electronics engineering*. https://doi.org/10.1002/047134608x.w8203

Wei, K., Li, J., Wang, L., Xing, Z., & Xu, R. (2016a). S-shaped periodic defected ground structures to reduce microstrip antenna array mutual coupling. *Electronics Letters*, *52*(15), 1288–1290. https://doi.org/10.1049/el.2016.0667

Wei, K., Li, J. Y., Wang, L., Xing, Z. J., & Xu, R. (2016b). Mutual coupling reduction by novel fractal defected ground structure bandgap filter. *IEEE Transactions on Antennas and Propagation*, *64*(10), 4328–4335. https://doi.org/10.1109/TAP.2016.2591058

Wei, K., Li, J. Y., Wang, L., & Xu, R. (2017). Microstrip antenna array mutual coupling suppression using coupled polarisation transformer. *IET Microwaves, Antennas and Propagation*, *11*(13), 1836–1840. https://doi.org/10.1049/iet-map.2016.1154

Wen, D., & Xin-Liang, L. (2018). The 2 ∗ 1 microstrip antenna array with low coupling using periodic paperclip-shaped slots. Paper presented at *Proceedings of the 2018 7th International Conference on Computer and Communication Engineering* (pp. 5–8). ICCCE. https://doi.org/10.1109/ICCCE.2018.8539341

Weng, L. H., Guo, Y. C., Shi, X. W., & Chen, X. Q. (2008). An overview on defected ground structure. *Progress in Electromagnetics Research B*, *7*, 173–189. https://doi.org/10.2528/pierb08031401

Wu, D., Cheung, S. W., Li, Q. L., & Yuk, T. I. (2017). Decoupling using diamond-shaped patterned ground resonator for small MIMO antennas. *IET Microwaves, Antennas and Propagation*, *11*(2), 177–183. https://doi.org/10.1049/iet-map.2016.0400

Wu, L., Lyu, H., & Yu, H. (2019a). A novel compact UWB-MIMO antenna with quintuple notched-band characteristics. *Wireless Personal Communications*, *108*(3), 1827–1840. https://doi.org/10.1007/s11277-019-06498-5

Wu, L., Lyu, H., Yu, H., & Xu, J. (2019b). Design of a miniaturized UWB-MIMO antenna with four notched-band characteristics. *Frequenz*, *73*(7–8), 245–252. https://doi.org/10.1515/freq-2018-0227

Wu, L., Xia, Y., Cao, X., & Xu, Z. (2018). A miniaturized UWB-MIMO antenna with quadruple band-notched characteristics. *International Journal of Microwave and Wireless Technologies*, *10*(8), 870–876. https://doi.org/10.1017/S1759078718000508

Wu, W., Zhi, R., Chen, Y., Li, H., Tan, Y., & Liu, G. (2019c). A compact multiband MIMO Antenna for IEEE 802.11 a/b/g/n applications. *Progress in Electromagnetics Research Letters*, *84*, 59–65. https://doi.org/10.2528/pierl19031106

Wu, Y. T., & Chu, Q. X. (2014). Dual-band multiple input multiple output antenna with slitted ground. *IET Microwaves, Antennas and Propagation*, *8*(13), 1007–1013. https://doi.org/10.1049/iet-map.2013.0340

Yadav, D., Abegaonkar, M. P., Koul, S. K., Tiwari, V., & Bhatnagar, D. (2018). Two element band-notched UWB MIMO antenna with high and uniform isolation. *Progress in Electromagnetics Research M*, *63*, 119–129. https://doi.org/10.2528/PIERM17091106

Yang, C., Yao, Y., Yu, J., & Chen, X. (2012). Novel compact multiband MIMO antenna for mobile terminal. *International Journal of Antennas and Propagation*, *2012*, 691681. https://doi.org/10.1155/2012/691681

Yang, D. G., Kim, D. O., & Kim, C. Y. (2014). Design of dual-band MIMO monopole antenna with high isolation using slotted CSRR for WLAN. *Microwave and Optical Technology Letters*, *56*(10), 2252–2257. https://doi.org/10.1002/mop.28574

Yang, Y., Chu, Q., & Mao, C. (2016a). Multiband MIMO antenna for GSM, DCS, and LTE indoor applications. *IEEE Antennas and Wireless Propagation Letters*, *15*, 1573–1576. https://doi.org/10.1109/LAWP.2016.2517188

Yang, Z., Li, F., & Li, F. (2018). A compact slot MIMO antenna with band-notched characteristic for UWB application. Paper presented *2018 International Conference on Microwave and Millimeter wave Technology (ICMMT 2018)-Proceedings* (pp. 1–3). https://doi.org/10.1109/ICMMT.2018.8563476

Yang, Z., Xiao, J., & Ye, Q. (2020). Enhancing MIMO antenna isolation characteristic by manipulating the propagation of surface wave. *IEEE Access*, *8*, 115572–115581. https://doi.org/10.1109/ACCESS.2020.3004467

Yang, Z.-X., Yang, H.-C., Hong, J.-S., & Li, Y. (2016b). A miniaturized triple band-notched MIMO antenna for UWB application. *Microwave and Optical Technology Letters*, *58*(3), 642–647. https://doi.org/10.1002/mop.29639

Yoon, H. K., Yoon, Y. J., Kim, H., & Lee, C. H. (2011). Flexible ultra-wideband polarisation diversity antenna with band-notch function. *IET Microwaves, Antennas and Propagation*, *5*(12), 1463–1470. https://doi.org/10.1049/iet-map.2010.0126

Yu, C., Yang, S., Chen, Y., Wang, W., Zhang, L., Li, B., & Wang, L. (2020). A super-wideband and high isolation MIMO antenna system using a windmill-shaped decoupling structure. *IEEE Access*, *8*, 115767–115777. https://doi.org/10.1109/ACCESS.2020.3004396

Zeng, Q., Yao, Y., Liu, S., Yu, J., Xie, P., & Chen, X. (2012). Tetraband small-size printed strip MIMO antenna for mobile handset application. *International Journal of Antennas and Propagation*, *2012*, 320582. https://doi.org/10.1155/2012/320582

Zhai, H., Ma, Z., Li, Z., & Liang, C. (2013). Reduction of mutual coupling between PIFA antennas for dual-band WiMAX operations. *Microwave and Optical Technology Letters*, *55*(10), 2321–2324. https://doi.org/10.1002/mop.27867

Zhang, J., Yan, S., Hu, X., & Vandenbosch, G. A. E. (2020). Mutual coupling suppression for on-body multiantenna systems. *IEEE Transactions on Electromagnetic Compatibility*, *62*(4), 1045–1054. https://doi.org/10.1109/TEMC.2019.2936679

Zhang, J. Y., Zhang, F., Tian, W. P., & Luo, Y. L. (2015). ACS-fed UWB-MIMO antenna with shared radiator. *Electronics Letters*, *51*(17), 1301–1302. https://doi.org/10.1049/el.2015.1327

Zhang, S., Lau, B. K., Tan, Y., Ying, Z., & He, S. (2012). Mutual coupling reduction of two PIFAs with a T-shape slot impedance transformer for MIMO mobile terminals. *IEEE Transactions on Antennas and Propagation*, *60*(3), 1521–1531. https://doi.org/10.1109/TAP.2011.2180329

Zhang, S., Ying, Z., Xiong, J., & He, S. (2009). Ultrawideband MIMO/diversity antennas with a tree-like structure to enhance wideband isolation. *IEEE Antennas and Wireless Propagation Letters*, *8*, 1279–1282. https://doi.org/10.1109/LAWP.2009.2037027

Zhao, Y., Zhang, F., Cao, L., & Li, D. (2019). A compact dual band-notched MIMO diversity antenna for UWB wireless applications. *Progress in Electromagnetics Research C*, *89*, 161–169. https://doi.org/10.2528/PIERC18111902

Zhou, X., Quan, X. L., & Li, R. L. (2012). A dual-broadband MIMO antenna system for GSM/UMTS/LTE and WLAN handsets. *IEEE Antennas and Wireless Propagation Letters*, *11*, 551–554. https://doi.org/10.1109/LAWP.2012.2199459

Zhu, J., Feng, B., Peng, B., Deng, L., & Li, S. (2016a). A dual notched band MIMO slot antenna system with Y-shaped defected ground structure for UWB applications. *Microwave and Optical Technology Letters*, *58*(3), 626–630. https://doi.org/10.1002/mop.29632

Zhu, J., Feng, B., Peng, B., Li, S., & Deng, L. (2016b). Compact CPW UWB diversity slot antenna with dual band-notched characteristics. *Microwave and Optical Technology Letters*, *58*(4), 989–994. https://doi.org/10.1002/mop.29714

Zhu, J., Li, S., Feng, B., Deng, L., & Yin, S. (2016c). Compact dual-polarized UWB quasi-self-complementary MIMO/diversity antenna with band-rejection capability. *IEEE Antennas and Wireless Propagation Letters*, *15*, 905–908. https://doi.org/10.1109/LAWP.2015.2479622

Zuo, S. L., Yin, Y. Z., Wu, W. J., Zhang, Z. Y., & Ma, J. (2010). Investigations of reduction of mutual coupling between two planar monopoles using two λ/4 slots. *Progress in Electromagnetics Research Letters*, *19*, 9–18. https://doi.org/10.2528/PIERL10100609